Journal Pre-proof

Identification and optimization of Piperlongumine analogues as potential antioxidant and anti-inflammatory agents via activation of Nrf2

Limei Ji, Lailiang Qu, Cheng Wang, Wan Peng, Shang Li, Huali Yang, Heng Luo, Fucheng Yin, Dehua Lu, Xingchen Liu, Lingyi Kong, Xiaobing Wang

PII: S0223-5234(20)30937-5

DOI: https://doi.org/10.1016/j.ejmech.2020.112965

Reference: EJMECH 112965

To appear in: *European Journal of Medicinal Chemistry*

Received Date: 28 August 2020

Revised Date: 14 October 2020

Accepted Date: 21 October 2020

Please cite this article as: L. Ji, L. Qu, C. Wang, W. Peng, S. Li, H. Yang, H. Luo, F. Yin, D. Lu, X. Liu, L. Kong, X. Wang, Identification and optimization of Piperlongumine analogues as potential antioxidant and anti-inflammatory agents via activation of Nrf2, *European Journal of Medicinal Chemistry*, https://doi.org/10.1016/j.ejmech.2020.112965.

This is a PDF file of an article that has undergone enhancements after acceptance, such as the addition of a cover page and metadata, and formatting for readability, but it is not yet the definitive version of record. This version will undergo additional copyediting, typesetting and review before it is published in its final form, but we are providing this version to give early visibility of the article. Please note that, during the production process, errors may be discovered which could affect the content, and all legal disclaimers that apply to the journal pertain.

© 2020 Elsevier Masson SAS. All rights reserved.

Graphical abstract:

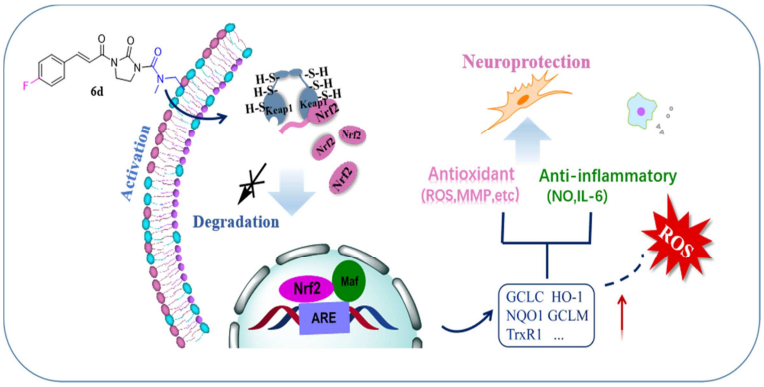

Journal Pre-proof

Journal Pre-proof

Identification and optimization of Piperlongumine analogues as potential antioxidant and anti-inflammatory agents via activation of Nrf2

Limei Ji, Lailiang Qu, Cheng Wang, Wan Peng, Shang Li, Huali Yang, Heng Luo, Fucheng Yin, Dehua Lu, Xingchen Liu, Lingyi Kong*, Xiaobing Wang *

Jiangsu Key Laboratory of Bioactive Natural Product Research and State Key Laboratory of Natural Medicines, Department of Natural Medicinal Chemistry, School of Traditional Chinese Pharmacy, China Pharmaceutical University, Nanjing 210009, China

*Corresponding Authors.

Tel/Fax: +86-25-83271405;

E-mail: xbwang@cpu.edu.cn (Xiaobing Wang); cpu_lykong@126.com (Lingyi Kong)

Journal Pre-proof

Journal Pre-proof

Abstract

Oxidative stress and inflammation are significant risk factors for neurodegenerative disease. The Keap1-Nrf2-ARE pathway is one of the most promising defensive systems against oxidative stress. Here, dozens of piperlongumine analogues were designed, synthesized, and tested on PC12 cells to examine neuroprotective effects against H_2O_2 and 6-OHDA induced damage. Among them, **6d** was found to be able to alleviate the accumulation of ROS, inhibit the production of NO and downregulate the level of IL-6, which indicated its potential antioxidant and anti-inflammatory activity. Further studies proved that **6d** could activate Nrf2 signaling pathway, induce the translocation of Nrf2 from cell cytosol to nucleus and upregulate the related phase II antioxidant enzymes including NQO1, HO-1, GCLC, GCLM and TrxR1. These results confirmed that **6d** exerted antioxidant and anti-inflammatory activities by activating Nrf2 signaling pathway. Moreover, the parallel artificial membrane permeability assay indicated that **6d** can cross the blood-brain barrier. In general, **6d** is promising for further development as a therapeutic drug against oxidative stress and inflammation related neurodegenerative disorders.

Keywords: Piperlongumine analogues; Oxidative stress; Neuroprotective effect; Keap1-Nrf2-ARE pathway

Journal Pre-proof

1. Introduction

Neurodegenerative diseases (ND), including Alzheimer's disease (AD), Parkinson's disease (PD), and multiple Sexual sclerosis (MS), are general term for diseases caused by chronic progressive degeneration of central nervous tissue [1 - 3]. These diseases have a common pathological feature, such as changes in the tissue redox balance accompanied by the activation of microglial cells [4]. The pathological processes of neurodegenerative diseases are associated with generation of reactive oxygen species (ROS), which cause oxidative stress [5]. Oxidative stress is supposed to play a key role in the development and progression of various diseases [5, 6]. For AD, oxidative stress can aggravate the deposition of Aβ and phosphorylation of tau protein, and promote Aβ and tau-mediated neurotoxicity. Furthermore, the presence of Aβ and tau is also resulted in the increase of ROS [6, 7]. These consequences, however, will further aggravate the oxidative stress response, which forms a vicious circle. Moreover, oxidative stress leads to cellular dysfunction and demise, especially playing a major role in the degeneration of dopaminergic neurons in the pathogenesis of PD [8]. Consequently, preventing ROS production and reducing oxidative stress may be a crucial therapeutic target for ND treatment.

The Keap1-Nrf2-ARE system plays a key role in antioxidant and anti-inflammatory mechanisms, which is one of the main cellular defense mechanisms against oxidative stress. As a dominant regulator in cell, Nrf2 fights against oxidative stress by activating anti-oxidative stress proteins, such as NQO1, GCLM, TrxR1, HO-1, and GCLC, and phase II detoxification enzymes [8 - 11]. Recently, related studies have

Journal Pre-proof

shown that the Keap1-Nrf2-ARE pathway could be rapidly activated during the development of neurodegenerative diseases [12], which is related to the production of ROS. In addition, Nrf2 also regulates the expression of HO-1 to achieve anti-inflammatory effect [13, 14]. In recent years, crystal structure of Keap1-sulfhydryl composite has been published, and covalent modification of cysteine-rich Keap1 protein by electrophilic molecules becomes an important strategy for the activation of Nrf2 [14]. The modulators are classified into Michael acceptors, polyenes, isothiocyanates, oxidizable, organosulfur compounds, trivalent arsenicals, diphenols, heavy metal species and selenium-containing compounds [15]. Dimethyl fumarate (Tecfidera) is the first Nrf2-inducer approved by FDA for the treatment of remitting-relapsing multiple sclerosis [16, 17]. Thus, chemicals with an electrophilic scaffold, especially α, β-unsaturated ketone structure, might be potent activators of Nrf2 [18, 19]. Many natural products, such as resveratrol [20], butein [21], caffeic acid [22] and curcumin [23], exhibit the potential to activate Nrf2. These scaffolds could covalently bind to cysteine residues of Keap1, resulting in dissociation of Nrf2 from Keap1, and translocation of Nrf2 from cytosol to the nucleus [24].

Piperlongumine (PL) is an alkaloid isolated from long pepper [25]. According to previously published studies, PL could increase the ROS level in cancer cells [26]. Researchers have found that PL has protective effect against AD, such as lowering cholinesterase levels, reducing neuroinflammation and inhibiting amyloid plaque formation [27, 28]. Based on the previous research, several general structure-activity relationships (SAR) have been identified. It reveals that the presence of 7, 8-olefin is

required. In addition, studies have shown that 2-chloro substitution may increase the electrophilicity of 2, 3-olefins, thereby enhancing activity [29, 30]. But few modifications on the position 2 and the lactam ring of PL were reported. In this study, the lactam ring, the position 2 of PL, and the aromatic ring were changed to study the SAR of PL. We reported herein the design, synthesis and biological evaluation of a series of PL analogues.

2. Results and discussion

2.1 Chemistry

PL analogues were synthesized by coupling acyl chlorides and commercially available lactams (**Scheme 1**) according to the published procedures with minor modifications [10]. All target compounds were characterized by ^{1}H NMR, ^{13}C NMR, and HRMS.

Scheme 1. Synthesis of PL analogs [a]

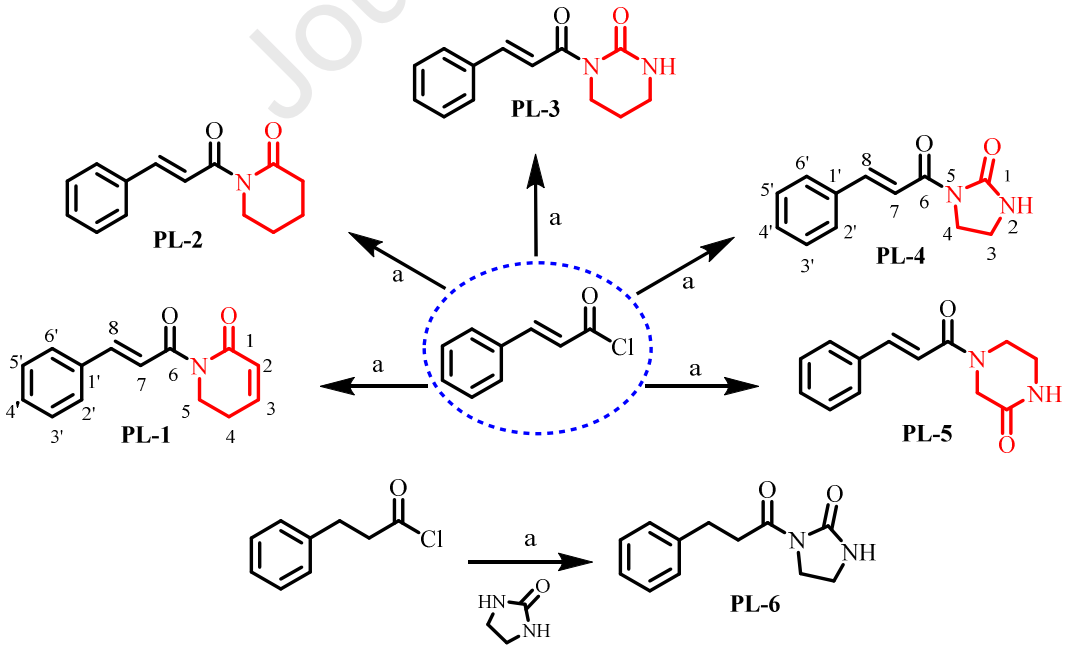

Journal Pre-proof

Journal Pre-proof

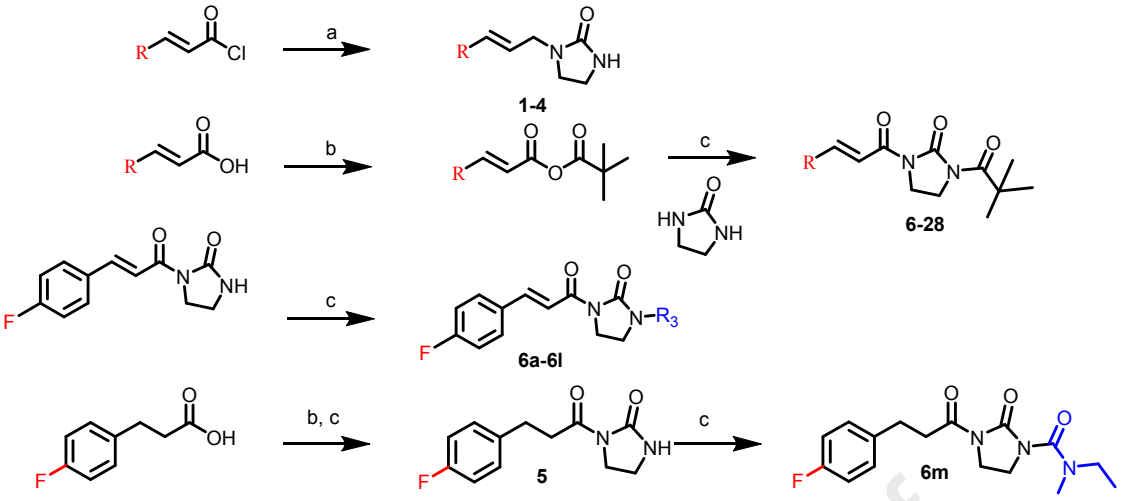

[a] Reagents and conditions: (a) NaH, THF, 0 °C, 30 min; (b) Trimethylacetyl chloride, TEA, DCM, 0 °C, 30 min; (c) NaH, DCM, 0 °C, 30 min.

2.2 Protection of PC12 cells against H_2O_2- and 6-OHDA-induced cell damage by PL analogues

The cytotoxicity of all compounds toward the PC12 cells were determined by the MTT assay. As shown in **Figure S2**, **PL**, **PL-1**, **6a**, **6b**, **6i** and **6l** displayed significant toxicity to the cells at high concentration (50 μM), and there were no apparent toxicity of the other tested compounds toward the PC12 cells at 50 μM. Two classic cellular models, 6-OHDA and H_2O_2 induced PC12 cell damage models, were established to evaluate the neuroprotective effect of the target compounds [30]. The specific concentration of H_2O_2 (200 μM) and 6-OHDA (150 μM) were chosen for the further study, where cell viability was approximately 50%. (**Figure S1)**.

The biological evaluation suggested that the 2, 3-position Michael acceptor moiety in PL could increase the cytotoxicity. When the *carbon atom* of the lactam ring of PL was replaced by the *nitrogen atom*, such as **PL-3** which showed better neuroprotection activity than that of **PL-2**. It was concluded that removing the α,

β-unsaturated in δ-valerolactam ring of PL could improve the neuroprotection. As expected, **PL-4** displayed lower cytotoxicity (**Figure S2A**) and better protection (**Figure 1**) in the initial screening. Few studies report the antioxidant activity of PL by replacing its lactam ring with 2-imidazolidone structures. We paid our attention on the modifications of the PL lactam with substituted imidazolidones, and **PL-4** was selected as a leading compound for the follow-up studies.

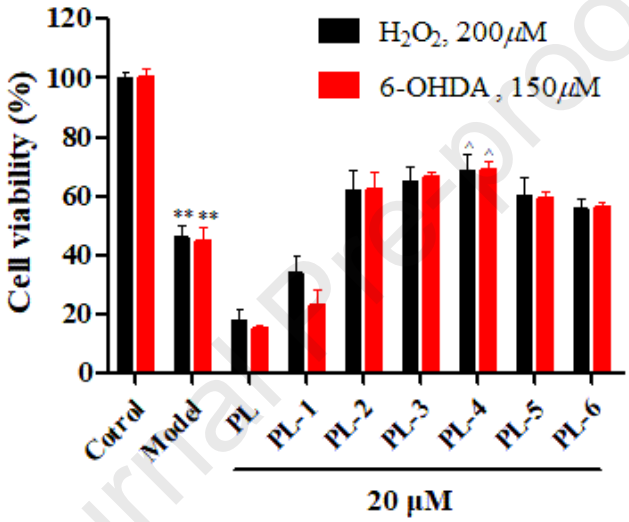

Figure 1 Initial screening of PL analogues against 6-OHDA- or H_2O_2-induced PC12 cell damage. Data are the mean ± SD of three independent experiments. (**p) ≤ 0.01 compared with the control group; (^p) ≤ 0.05 compared with H_2O_2-treated or 6-OHDA-treated group.

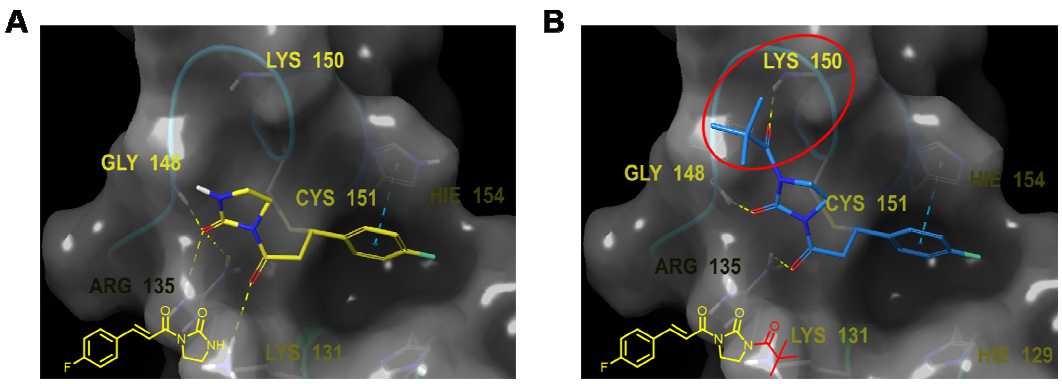

Journal Pre-proof

Figure 2. The docking models of icompond **1** (A) and **6** (B) with the BTB domain of Keap1 (PDB: 4CXT).

Glide program in Schrodinger was utilized to predict the potential binding model between **1** and Keap1 BTB domain (**Figure 2A**). The covalent docking results showed that **1** could form a covalently bond with residue CYS151 of Keap1, the benzene ring from **1** formed π-π stacking with residue HIE154, and the carbonyl group from the α, β-unsaturated ketone and the lactam carbonyl group formed hydrogen bonds with residues GLY148, LYS131 and GLY145. The docking results displayed that the residue LYS150 as a hydrogen bond donor around the interface pocket is very close to the ligand. With this in mind, compound **6** having a hydrogen bond acceptor was designed, and the docking result showed that the added pivaloyl fragment did form hydrogen bond with residue LYS150 (**Figure 2B)**. In this point, compounds **1**, **2**, **3** and **4** without pivaloyl and compounds **6**, **15**, **20** and **21** with pivaloyl were designed and synthesized. The experimental results showed that the added pivaloyl play crucial roles in their neuroprotective activities (**6**, **15**, **20** and **21** vs. **1**, **4**, **3** and **2**, **Tables 1** and **2**). To further verify the influence of added pivaloyl to the expression of Nrf2. PC12 cells were treated with compounds **1** and **6** for 24 h, and the expression of Nrf2 was detected by western blot. As showed in **Figure 3**, the expression of Nrf2 was significantly upregulated, and the upregulation of Nrf2 by **6** was more obvious than that of compound **1**. The results suggested that the pivaloyl group is vital to activate Nrf2.

To validate the SAR, a variety of additional aryl analogues (**1 - 28**) with different benzyl groups varying from *para* and *ortho* to *meta* substituents were synthesized

Journal Pre-proof

(**Tables 1** and **2**). All the target compounds showed negligible cytotoxicity (**Figure S2A**). Different substituted groups were introduced to phenyl. The 4'-F substituted compound **6** exhibited potent neuroprotection with cell viability (73.58%) better than that of **14** and **13** (4'-F > 2'-F > 3'-F). The 4'-Cl substituted **8** exhibited potent neuroprotection better than that of **17** and **18** (4'-Cl > 2'-Cl > 3'-Cl). It is well known that the majority nature of heterocycles is served as hydrogen bond donors and receptors. In this study, heterocycles were utilized to replace the aromatic group in the scaffold of PL. Several compounds substituted by furan **(20)**, thiophene **(21)**, pyridine **(22)**, naphthalene **(24)**, 1, 3-benzodioxole **(25)** were synthesized. Unfortunately, the neuroprotection was not improved compared to the compounds containing phenyl. Among the tested compounds, the compounds with electron-withdrawing groups showed better neuroprotective activity than that with the electron-donating groups. The monosubstituted compounds **6** (73.58%), **13** (70.97%) and **14** (72.43%) show better neuroprotective activity than the polysubstituted compounds **16** (63.55%) and **26** (59.15%). It is remarkable that **6** showed best protection against 6-OHDA and H_2O_2 induced PC12 cell damage (**Tables 1** and **2**).

Table 1 The neuroprotection of PL analogues substituted with different aryl group

Compd.	Structure	Cell viability (%)	
		H_2O_2	6-OHDA
Model		46.00 ± 4.12	45.23 ± 4.37
1	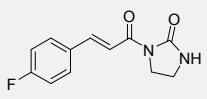	68.57 ± 2.88	69.13 ± 3.4

2	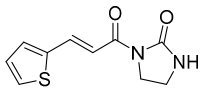	65.15 ± 3.86	64.2 ± 1.74
3	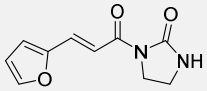	64.08 ± 3.55	60.00 ± 2.72
4	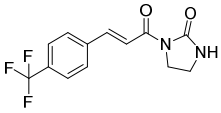	67.66 ± 4.15	65.32 ± 4.72
5	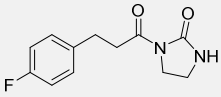	53.56 ± 1.29	56.32 ± 2

[a] Cell viability (%) of PC12 cells were detected by the MTT assay after 24 h of incubation with compounds at the concentration of 20 μM with H_2O_2 (200 μM) or 6-OHDA (150 μM). Data are the mean ± SD of three independent experiments.

Table 2 The neuroprotection of PL analogues substituted with different aryl group

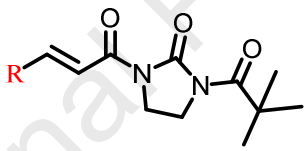

Compd.	R	Cell viability (%)[a]		Compd.	R	Cell viability (%)	
		H_2O_2	6-OHDA			H_2O_2	6-OHDA
Model		46.00 ± 4.12	45.23 ± 4.37	**17**		70.01 ± 4.55	69.01 ± 2.39
6	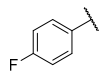	73.58 ± 3.55	72.23 ± 2.72	**18**		69.21 ± 1.87	68.32 ± 4.06
7	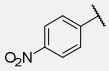	70.15 ± 3.86	69.21 ± 0.74	**19**		60.36 ± 2.42	56.73 ± 1.30
8	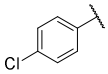	72.05 ± 2.15	71.12 ± 3.23	**20**		69.66 ± 4.15	68.31 ± 4.72
9	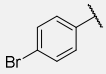	72.22 ± 2.11	70.79 ± 2.82	**21**		69.23 ± 3.86	68.21 ± 4.55
10	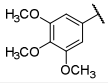	72.1 8 ± 0.76	72.32 ± 2.25	**22**		70.91 ± 5.32	69.58 ± 2.51
11	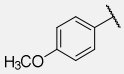	71.14 ± 1.81	70.32 ± 3.09	**23**		71.41 ± 4.5	71.12 ± 4.02

12	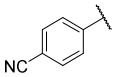	61.52 ± 3.22	60.08 ± 5.27	**24**		72.33 ± 3.54	71.79 ± 5.49
13		70.97 ± 2.54	69.32 ± 4.19	**25**	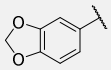	63.33 ± 1.05	62.31 ± 2.94
14		72.43 ± 2.54	72.33 ± 1.20	**26**		59.15 ± 4.34	56.38 ± 5.36
15	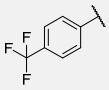	72.5 ± 2.88	71.12 ± 3.40	**27**	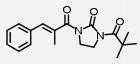	73.22 ± 2.73	72.13 ± 6.40
16	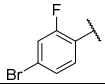	63.55 ± 1.64	61.77 ± 2.54	**28**	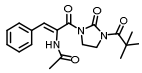	72.65 ± 4.48	71.21 ± 2.62

[a] Cell viability (%) of PC12 cells were detected by the MTT assay after 24 h of incubation with compounds at the concentration of 20 μM with H_2O_2 (200 μM) or 6-OHDA (150 μM). Data are the mean ± SD of three independent experiments.

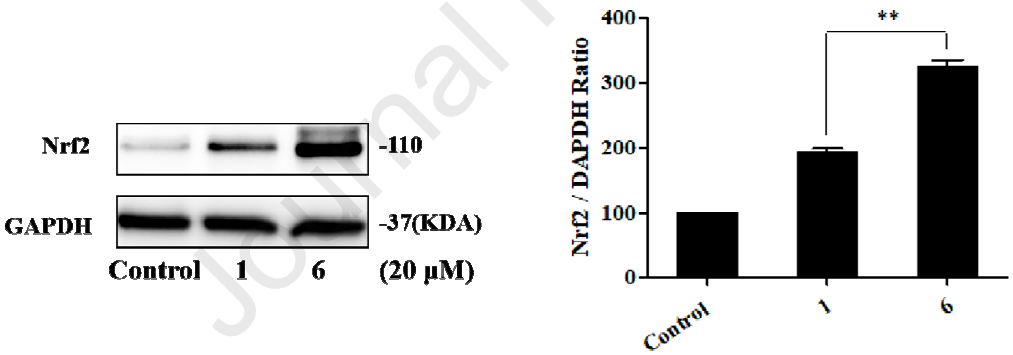

Figure 3 The expression of Nrf2 in PC12 cells after treatment with compounds **1** and **6.** (**p) ≤ 0.05, Data are presented by mean ± SD (n = 3).

As exhibited in **Table 3**, compounds **6a**, **6b**, **6i**, and **6l** displayed obvious cytotoxicity at low concentrations (**Figure S2B**). In addition, their neuroprotective effect were eliminated or weakened, which may be related to their toxicity. When the position 2 of *N*-terminus was connected to the aromatic structure, such as **6k**, **6l** and **6j**, the neuroprotective effects of them were reduced. When carbonyl was connected to

Journal Pre-proof

piperidine (**6e**), *N*, *N*-dimethyl (**6c**) and *N*-methyl, *N*-ethyl (**6d**), the neuroprotective effects were significantly enhanced. It is remarkable that **6d** showed excellent neuroprotective effect (75.01%). To verify whether α, β-unsaturated ketone is an essential group for neuroprotection, compounds **PL-6**, **5** and **6m** were synthesized and evaluated their neuroprotective effects. As expected, compounds **PL-4** (68.80%), **1** (68.57%) and **6d** (75.01%) exhibited potency neuroprotective effect with cell viability better than that of **PL-6** (55.78%), **5** (53.56%) and **6m** (59.50%), respectively. In general, we synthesized a series of **PL** analogues following the strategy shown in **Figure 4** and evaluated their neuroprotective activities. Among them, **6d** showed lower cytotoxicity (**Figure S2B**), best neuroprotective effect (**Table 3**), and was chosen for the follow-up studies.

Table 3 The neuroprotection of **PL** analogues substituted with different groups

Compd.	**Structure**	**Cell viability (%)[a]**	
		(H_2O_2-induced)	**(6-OHDA-induced)**
Model		46.96 ± 4.12	45.65 ± 4.37
6a	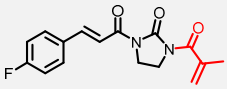	38.05 ± 3.20	30.23 ± 4.35
6b	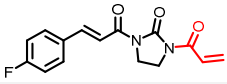	43.96 ± 5.43	43.76 ± 5.01
6c	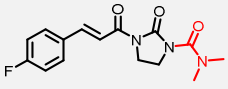	73.82 ± 1.39	71.32 ± 2.87
6d	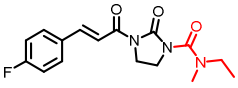	75.01 ± 2.02	75.44 ± 2.29
6e	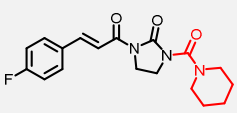	72.8 ± 1.19	72.14 ± 2.60

6f	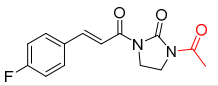	70.42 ± 4.51	72.27 ± 2.21
6g	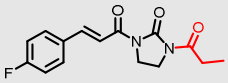	71.58 ± 4.55	70.23 ± 3.72
6h	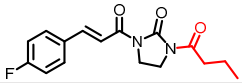	70.15 ± 3.86	69.26 ± 1.74
6i	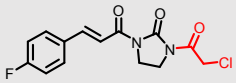	43.25 ± 4.15	37.12 ± 3.23
6j	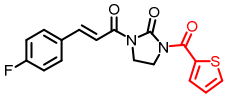	62.25 ± 2.11	60.79 ± 2.82
6k	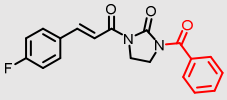	63.28 ± 0.76	60.32 ± 5.25
6l	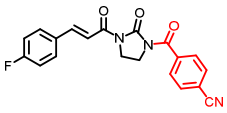	55.14 ± 4.81	52.32 ± 2.09
6m	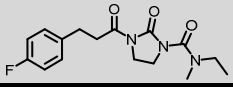	59.5 ± 4.20	62.45± 1.20

[a] Cell viability (%) of PC12 cells were detected by the MTT assay after 24 h of incubation with compounds at the concentration of 20 μM with H_2O_2 (200 μM) or 6-OHDA (150 μM). Data are the mean ± SD of three independent experiments.

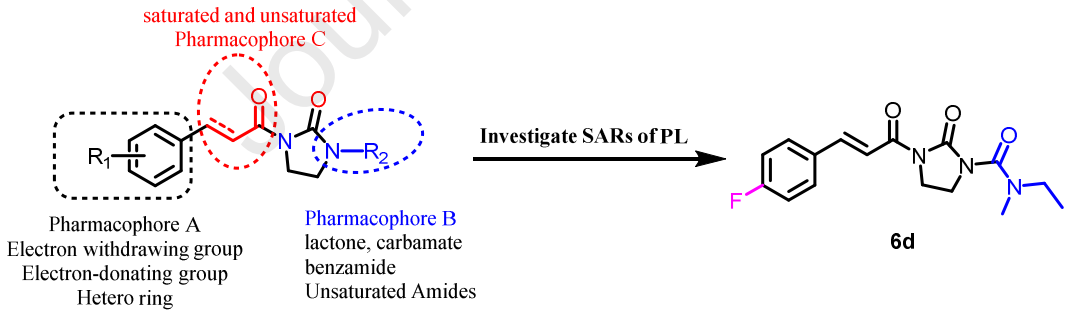

Figure 4 The design of the modifications of PL

2.3. Antioxidant effect of 6d

*2.3.1. Defense of PC12 Cells against H_2O_2 or 6-OHDA induced cell damage in a dose dependent manner by **6d***

Initially, we investigated the cytotoxicity of all compounds on the PC12 cells (a rat pheochromocytoma cell line), BV2 cells (mouse microglia), and L02 cells (an

Journal Pre-proof

immortal hepatic). As shown in **Figure S3**, no apparent toxicity was observed at 50 μM. In **Figures 5A** and **5B**, compared with control group, cells pretreated with **6d** (5, 10 and 20 μM) for 24 h followed by treatment with H_2O_2- and 6-OHDA exhibited stronger viability in dose-dependent manners. Lactate dehydrogenase (LDH) is an important indicator of membrane integrity [31]. To confirm the cytoprotection of **6d**, the content of LDH leakage after H_2O_2- or 6-OHDA-treated was determined. As shown in **Figures 5C** and **5D**, the content of LDH was up-regulated by H_2O_2 or 6-OHDA, and the release amount of LDH increased 2.8-fold and 1.8-fold that of the control respectively, which was the same as the expected result. After pretreatment with **6d**, the leakage of LDH was significantly reduced. The above results indicated that the non-toxic concentration of **6d** could prevent the neurotoxicity induced by H_2O_2 and 6-OHDA in PC12 cells.

Journal Pre-proof

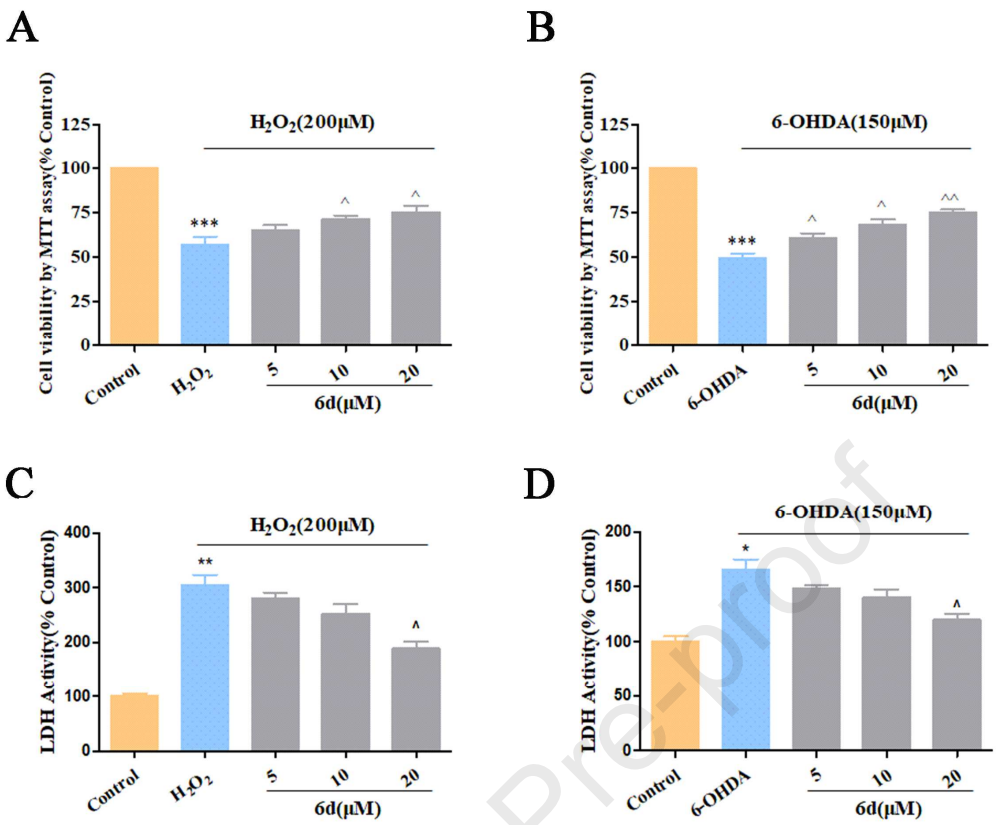

Figure 5. Protection of **6d** against H_2O_2- (A) and 6-OHDA-induced (B) PC12 cell damage, determined by MTT assay. Protection of **6d** against H_2O_2-induced (C) and 6-OHDA-induced (D) PC12 cell damage was measured by the LDH release assay. Data are the mean ± SD of three independent experiments. (**p) ≤ 0.01 and (***p) ≤ 0.001 compared with the control group; ($^{\wedge}$p) ≤ 0.05, ($^{\wedge\wedge}$p) ≤ 0.01 and ($^{\wedge\wedge\wedge}$p) ≤ 0.001 compared with H_2O_2-treated or 6-OHDA-treated group.

2.3.2 Prevention of ROS accumulation in PC12 cells

Oxidative stress response to ROS is a key initiator of oxidative damage induced by H_2O_2 and 6-OHDA. In order to study the protection of **6d** to the oxidative damage in PC12 cells, the level of ROS was quantified by dichlorofluorescein diacetate (DCFH-DA) using flow cytometry [32, 33]. When PC12 cells were exposed to H_2O_2 or

Journal Pre-proof

6-OHDA, the intracellular ROS fluorescence intensity increased significantly. However, when pretreated with an increasing concentration of **6d** (5, 10 and 20 μM), the ROS levels decreased in a dose-dependent manner (**Figures 6A** and **6B**). The result suggested that **6d** effectively reduced H_2O_2- and 6-OHDA-induced ROS accumulation.

*2.3.3 Alleviation of H_2O_2- and 6-OHDA-induced intracellular mitochondrial dysfunction by **6d***

Mitochondria are important mediators of cell metabolism and main producers of ROS. The reduction of mitochondrial membrane potential (MMP) is a sign of early apoptosis. The reduction of cell membrane potential can be detected by the red fluorescence of JC-1 converted to green fluorescence [34]. **Figures 6C** and **6D** showed that H_2O_2 and 6-OHDA reduced the MMP of PC12 cells, indicating that H_2O_2- and 6-OHDA caused the mitochondrial dysfunction. In contrast, pretreatment of PC12 cells with **6d** before exposure to H_2O_2 or 6-OHDA could significantly increase the MMP. These results showed that **6d** had potent protection against H_2O_2- or 6-OHDA-induced mitochondrial dysfunction in PC12 cells.

Journal Pre-proof

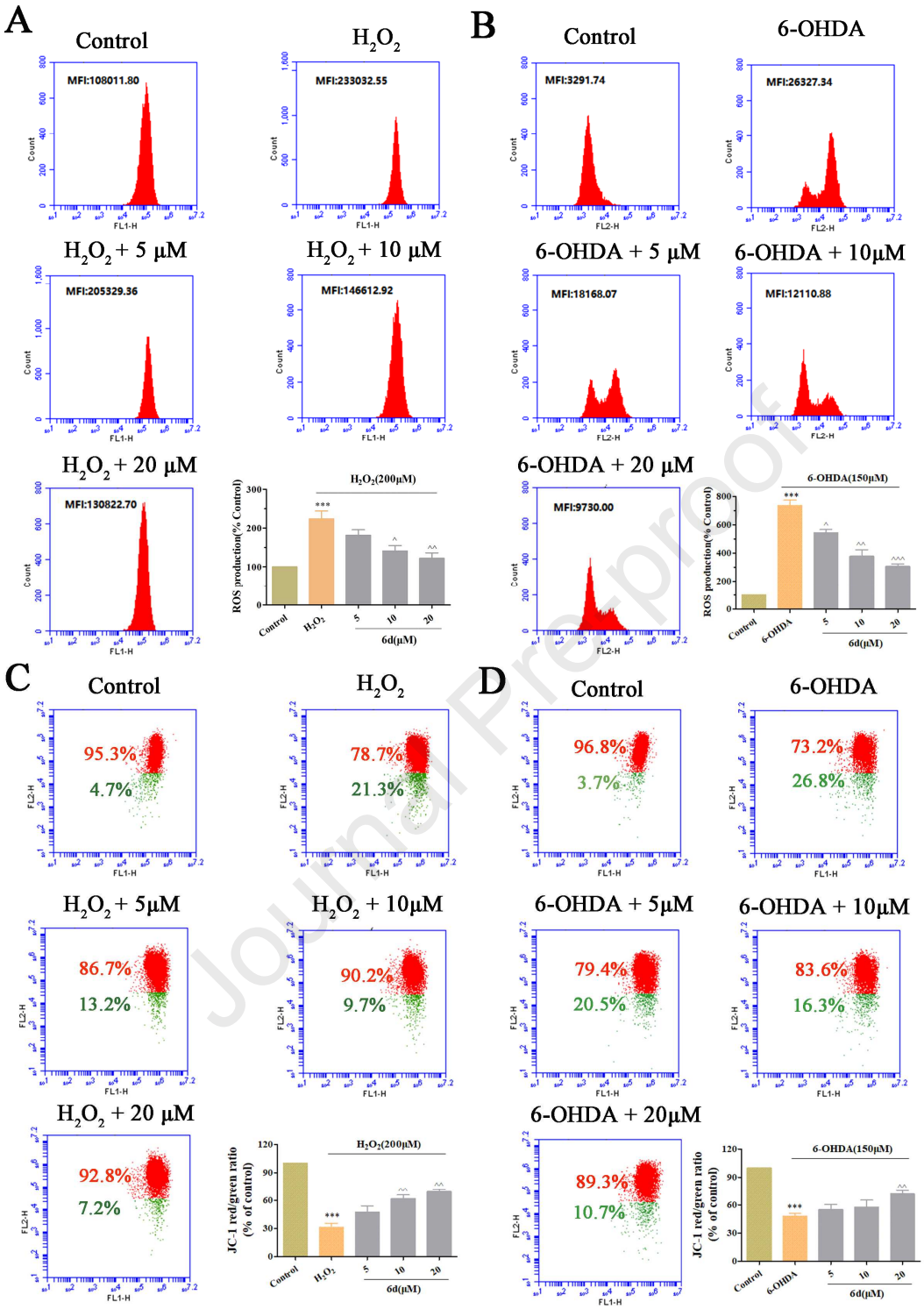

Figure 6. The effects of **6d** on H_2O_2-induced (A) and 6-OHDA-induced (B) intracellular ROS production in PC12 cells. The cells were stained with DCFH-DA and immediately determined by flow cytometry. The effects of **6d** on H_2O_2-induced (C)

and 6-OHDA-induced (D) MMP reduction in PC12 cells. MMP were detected by flow cytometry after JC-1 staining. Data are presented by mean ± SD (n = 3). (***p) ≤ 0.001 compared with the control group; (^p) ≤ 0.05, (^^p) ≤ 0.01 and (^^^p) ≤ 0.001 compared with H_2O_2-treated or 6-OHDA-treated group.

2.3.4 Alleviation of H_2O_2- and 6-OHDA-induced PC12 cell apoptosis

To investigate the anti-apoptosis ability of **6d** against H_2O_2- and 6-OHDA-*induced* cell damage, quantified Annexin V-FITC and propidium iodide (PI) were used to evaluate apoptotic cells by flow cytometry [35]. As shown in **Figure 7A**, compared with the control group, the apoptosis rate of PC12 cells increased from 5.71% (control group) to 25.38% (H_2O_2 treated group) after treatment with H_2O_2 for 24 h. In contrast, the rates of apoptotic cells were significantly reduced when H_2O_2-treated PC12 cells were co-incubated with **6d** (5, 10 and 20 μM), the cell apoptosis rate was reduced to 16.45%, 7.62%, and 6.52%, respectively. Similarly, in **Figure 7B**, the apoptosis rate of PC12 cells increased from 3.23% (control group) to 27.5% (6-OHDA treated group) after treatment with 6-OHDA for 24 h, and the cell apoptosis rate was reduced to 19.17%, 15.07%, and 10.83% after the cells were pretreated with **6d** (5, 10 and 20 μM).

Hoechst 33342 is a blue fluorescent dye that can penetrate cell membranes and is commonly used to detect apoptosis. After staining, images were captured using a high-content imaging system. As shown in **Figures 7C** and **7D**, both H_2O_2 and 6-OHDA could cause PC12 cell apoptosis. The apoptotic nuclei were characterized by highly fluorescent aggregates, while no obvious apoptotic nuclei were observed in the

control group. Pretreatment of cells with **6d** significantly reduced the number of apoptotic nuclei, which indicated that **6d** showed significant neuroprotective effect against H_2O_2- and 6-OHDA-induced apoptosis.

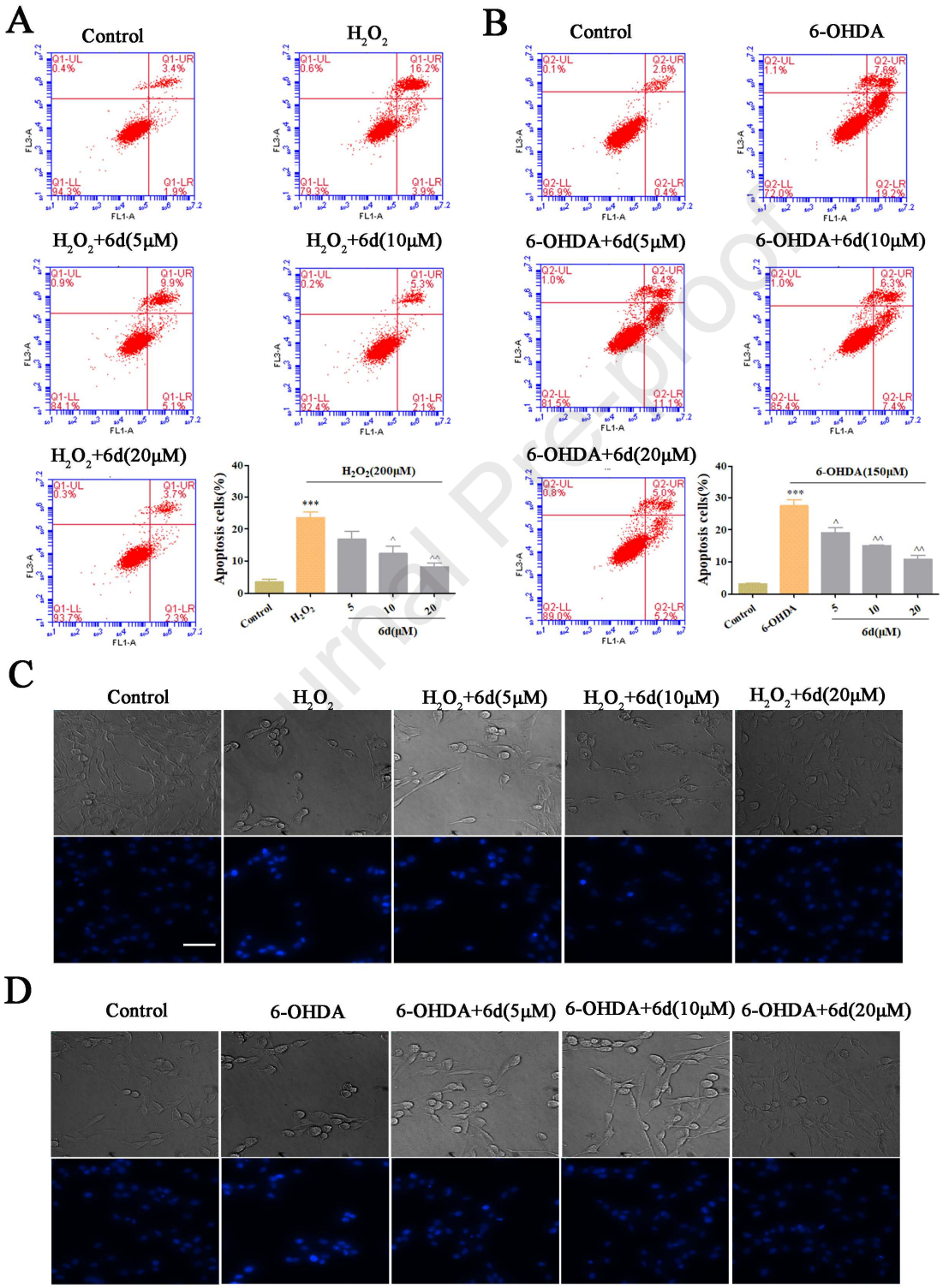

Figure 7. Prevention of PC12 cells from H_2O_2-induced (A) and 6-OHDA-induced (B)

apoptosis by **6d**. Apoptotic cells were detected by flow cytometry after AnnexinV and PI double staining. (C, D) Images showed the apoptotic nuclei by Hoechst 33342 staining. The top panel is phase contrast pictures, and the bottom panel is fluorescent pictures. Scale bars: 100 μm. Data are presented by mean ± SD (n = 3). (***p) ≤ 0.001 compared with the control group; (^p) ≤ 0.05 and (^^p) ≤ 0.01 compared with H_2O_2- or 6-OHDA-treated group.

*2.3.5 The reduction of H_2O_2-induced and 6-OHDA-induced Ca^{2+} overload on PC12 cells by **6d***

Increased ROS will react with cellular proteins, nucleic acids, *et al*., to cause cellular barriers to affect cellular Ca^{2+} influx. Ca^{2+} has been shown to mediate cytotoxicity of oxidative stress. Fluo-3 AM fluorescent probe can be used to detect the concentration of Ca^{2+} in the cell, and the relative intensity of Ca^{2+} is reflected by the fluorescence intensity [36, 37]. After being stimulated with H_2O_2 or 6-OHDA for 24 h, the intracellular Ca^{2+} was almost 3.3 times and 1.8 times, respectively (**Figures 8A, B**). Compared with the control group, the intracellular free Ca^{2+} fluorescence value increased from 5537.87 (control group) to 17791.36 (H_2O_2 treated group) after treatment with H_2O_2 for 24 h. In contrast, pretreatment of PC12 cells with **6d** (5, 10 and 20 μM) before exposure to H_2O_2 sharply dropped the intracellular free Ca^{2+} fluorescence value to 8721.73, 7793.41, and 6730.32, respectively. Similarly, the intracellular free Ca^{2+} fluorescence value increased from 3998.83 (control group) to 6708.18 (6-OHDA treated group) after treatment with 6-OHDA for 24 h. Pretreatment of PC12 cells with **6d** (5, 10 and 20 μM) before exposure to 6-OHDA significantly

dropped the intracellular free Ca^{2+} fluorescence value to 4910.91, 4204.33, and 4161.82, respectively. The experimental results showed that **6d** in PC12 cells could prevent 6-OHDA- or H_2O_2-induced Ca^{2+} overload. It was in agreement with the results of ROS, MMP and apoptosis above, which suggested that **6d** could be used as a potential neuroprotective agent for the treatment of ND.

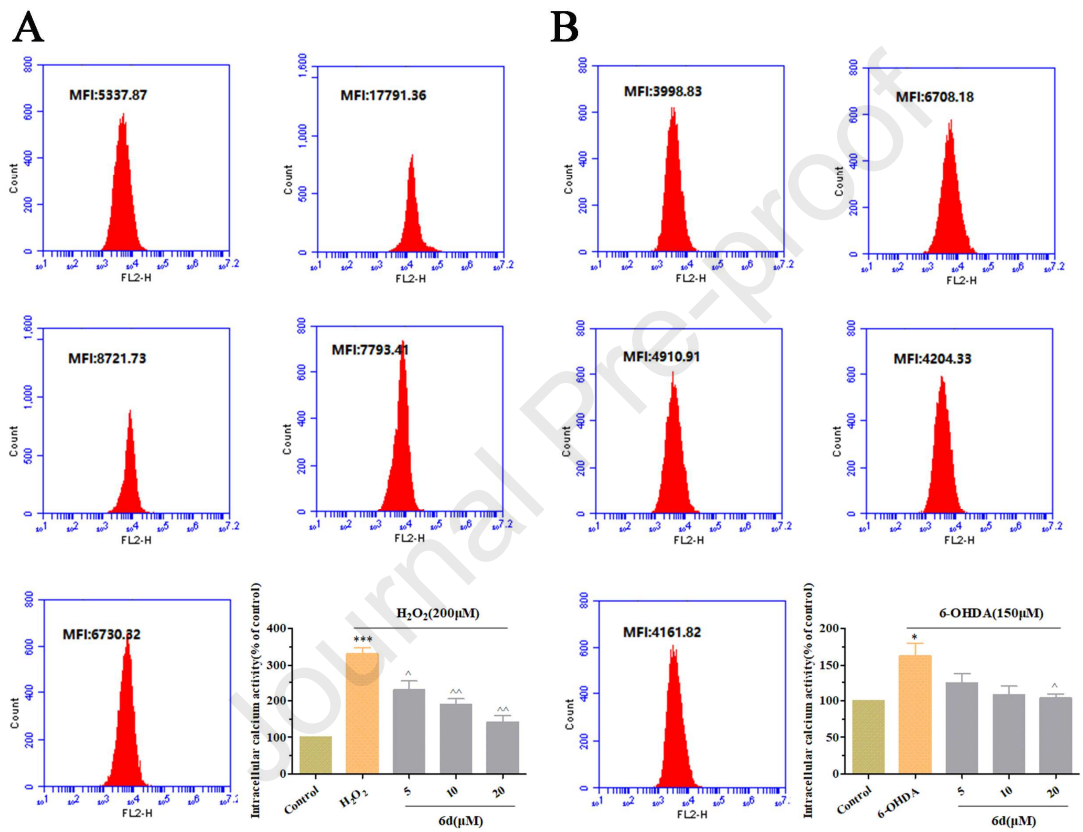

Figure 8. Effects of **6d** on H_2O_2-induced (A) and 6-OHDA-induced (B) Ca^{2+} overload in PC12 cells. Data are presented by mean ± SD (n = 3). (*p) ≤ 0.05 and (***p) ≤ 0.001 compared with the control group; ($^{\wedge}$p) ≤ 0.05 and ($^{\wedge\wedge}$p) ≤ 0.01 compared with H_2O_2-treated or 6-OHDA-treated group.

*2.3.6 The Activation of the Keap1-Nrf2-ARE Pathway and the Induction of the Downstream Antioxidant Proteins Expression in PC12 Cells by **6d***

As confirmed above, **6d** showed potent protection on PC12 cells against

Journal Pre-proof

313 6-OHDA- or H_2O_2-induced cell damage, alleviated ROS accumulation, mitochondrial
314 dysfunction, Ca^{2+} influx, and cell apoptosis. We hypothesized that the antioxidant
315 activitie of **6d** is related to the activation of Nrf2. To verify whether **6d** could activate
316 the Nrf2-Keap1-ARE pathway, the expression of Nrf2 and its downstream antioxidant
317 proteins were detected by Western blot. The protein level for Nrf2 was maximal after a
318 3 h treatment of with the highest concentration **6d** (20 μM), the protein levels for HO-1,
319 GCLM reached maximum at 12 h, and the protein levels for TrxR1, NQO1 and GCLC
320 reached maximum at 24 h (**Figure 9A**). Western blot analysis demonstrated that
321 treatment with **6d** for 24 h resulted in a remarkable increase of the Nrf2-regulated
322 proteins (NQO1, HO-1, TrxR1, GCLM, and GCLC) in a dose-dependent manner
323 (**Figure 9B**) [38].

324 DPPH (diphenyl-1-picrylhydrazyl) and ABTS radical scavenging method was
325 used to assess the antioxidant activities of these compounds in vitro，where Trolox was
326 used as a positive [39, 40]. **6d** is incapable of intercepting either DPPH or ABTS free
327 radicals (**Figure S4**), which indicated that **6d** exerted neuroprotective effect as an
328 activator rather than direct radical scavenger.

329 The translocation of Nrf2 from cytosol to nucleus is prerequisite for the
330 expression of Nrf2-dependent proteins. To confirm that whether **6d** could transfer Nrf2
331 from the cytoplasm to the nucleus. First, we checked the nuclear and cytoplasmic Nrf2
332 expression. Nuclear Nrf2 accumulation increased maximally at 6 h. Cytosol Nrf2
333 accumulation increased maximally at 3 h and declined after 6 h. These results indicated
334 that **6d** promoted the transfer of Nrf2 to the nucleus, which facilitates the binding of

Journal Pre-proof

Nrf2 to ARE for the transcription process. (**Figure 9C**) [41]. Besides, to confirm whether **6d** exerted the anti-inflammatory or antioxidant activity by activating Nrf2 signaling pathway, antioxidant assay was performed with the existence of Nrf2 inhibitor brusatol or the HO-1 inhibitor zinc protoporphyrin IX (ZnPP) existed [30]. As shown in **Figures 9D** and **9E**, **6d** alleviated the H_2O_2 or 6-OHDA induced cell death at 20 μM, while this neuroprotective effect was almost abolished in the group pretreated with brusatol or ZNPP. This result demonstrated that Nrf2 was essential for the neuroprotective effect of **6d** in PC12 cells.

Journal Pre-proof

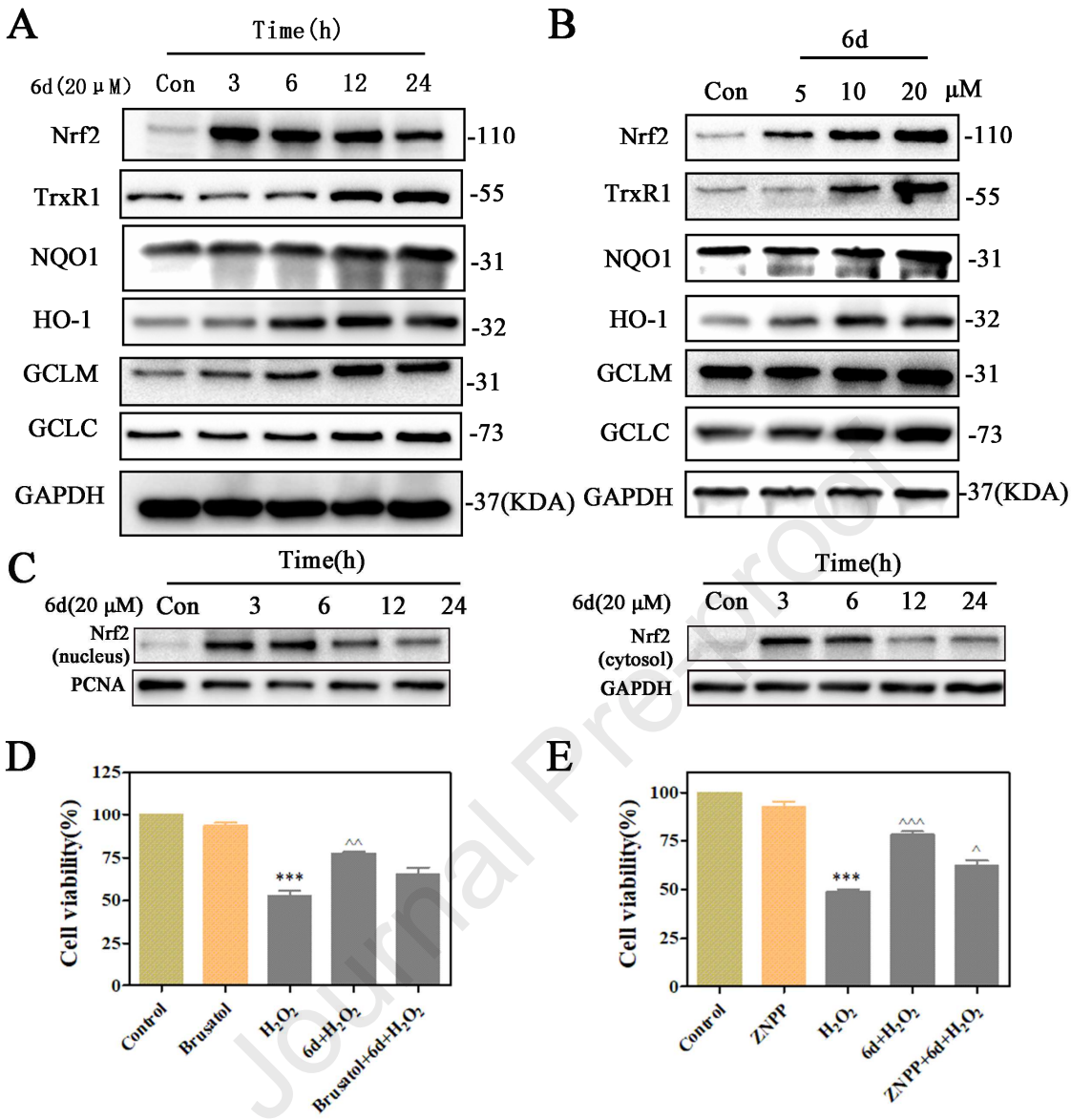

Figure 9. 6d could increase the expression of nuclear and cytosolic Nrf2, TrxR1, NQO-1, HO-1, GCLM and GCLC in a time (A) and dose (B) dependent manner. Promotion of Nrf2 nuclear accumulation by **6d** (C). Brusatol (D), ZnPP (E) affected the protection of **6d**. PC12 cells were incubated for 30 min in the presence of **6d** (20 μM) together with brusatol (10 nM) or ZNPP (10 nM) prior to stimulation with H_2O_2 (150 μM) for 24 h, determined by MTT assay. Data are presented by mean ± SD (n = 3).

Journal Pre-proof

2.4 Anti-inflammatory effect of 6d

The excessive activation of microglia plays an important part in neuronal damage and death caused by AD and PD neuroinflammation [42]. NO release is a vital feature of microglia activation. Excessive NO production can cause inflammation [43]. Besides, many researchers believe that HO-1 regulates the inflammatory process and is related to the Nrf2 / ARE pathway [44 - 46]. Collectively, activating Nrf2 is an excellent method to reduce the inflammatory process [46]. The anti-neuroinflammation property was measured using the Griess method to examine the effects of **6d** on the production of NO. The results showed that after the 18 h incubation with LPS (1μg/mL), the level of NO increased sharply compared to the control group. However, the levels of NO dose-dependently decreased when BV2 microglia cells were pretreated with **6d** before exposed to LPS (**Figure 10A**). It is well known that the release of inflammatory factors contributes to the development of inflammation. IL-6 is an important indicator to evaluate the activation degree of macrophages and the progress of inflammatory response [47, 48]. **6d** significantly attenuated LPS-induced production of IL-6 in BV2 microglia cells (**Figure 10B**). The potential anti-inflammatory effect may be related to the activation of the Nrf2 signaling pathway. We determined the expression of Nrf2 and its downstream anti-oxidant proteins using Western blot. As shown in **Figure 10C**, treatment of BV2 microglia cells with **6d** for 24h could significantly upregulate the expression of these proteins with dose dependent manner, which was similar with that in PC12 cells. Then, to investigate whether activation of Nrf2 is responsible for the anti-inflammatory effect of **6d**, Nrf2

Journal Pre-proof

was knockdown by siRNA. Then the control siRNA- and Nrf2 siRNA-transfected BV2 microglia cells were pre-treated with **6d** (20 μM) and stimulated with LPS for another 18 h. The level of Nrf2 decreased sharply in Nrf2 siRNA-transfected BV2 microglia cells (**Figure 10D**). Furthermore, **6d** (20 μM) could significantly reduce LPS-induced NO production in control siRNA-transfected BV2 microglia cells (**Figure 10E**) [49 - 51]. However, the suppressive effects of **6d** (μM) was obviously suppressed in Nrf2 siRNA-transfected BV2 microglia cells. Similar results were observed in experiments to determine the effects of Nrf2 knockout on the inhibition of IL-6 production (**Figure 10F**). These results demonstrated that **6d** exerted anti-inflammatory effect with a Nrf2-dependent manner in BV2 microglia cells.

Journal Pre-proof

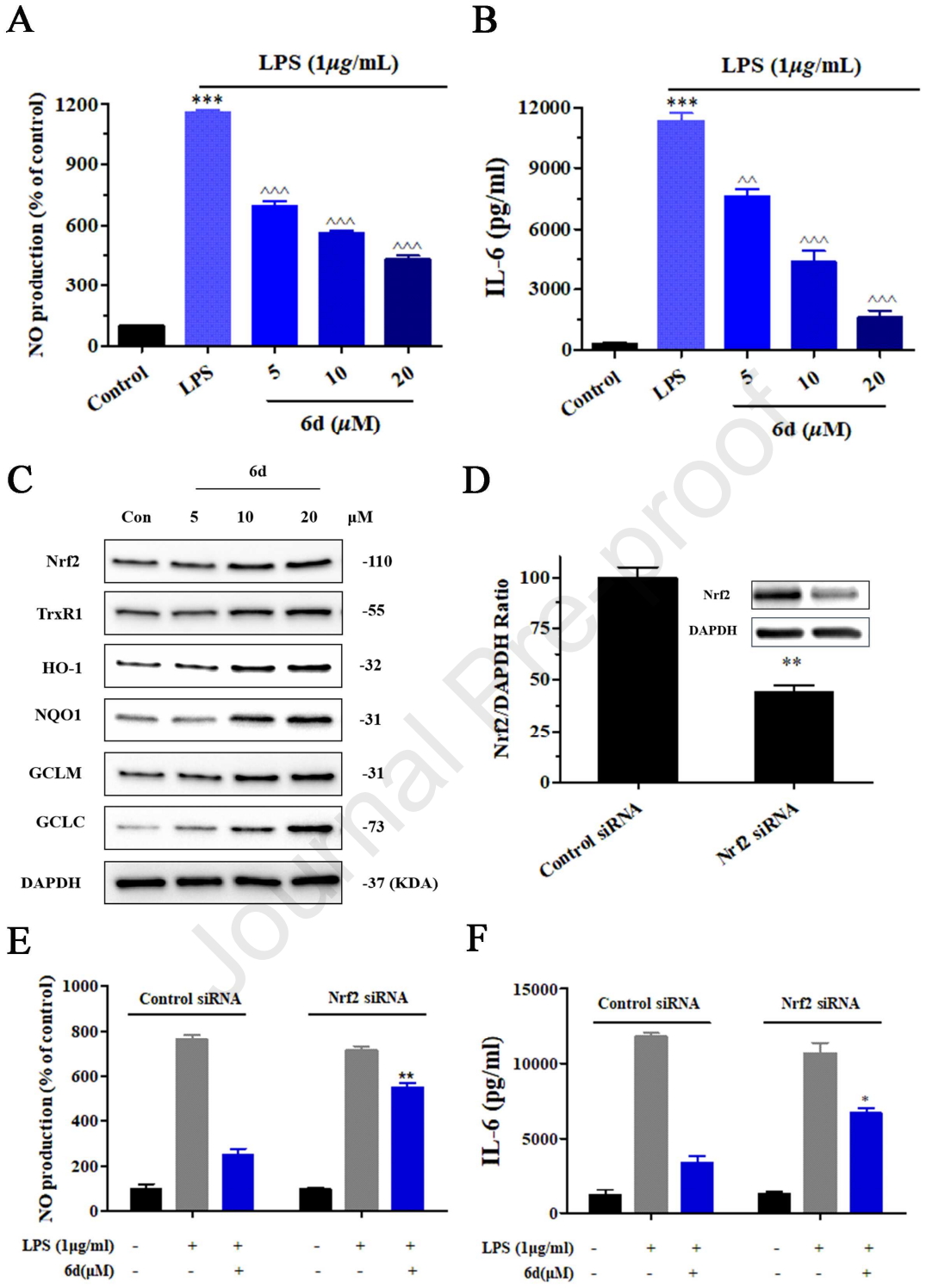

384

385 **Figure 10.** Contribution of Nrf2 to the anti-inflammatory effect of **6d**. (A) **6d** reduced

386 the production of LPS-stimulated inflammatory mediators NO in BV2 microglia cells.

387 (B) **6d** reduced the production of LPS-induced IL-6 in BV2 microglia cells. The levels

388 of IL-6 were measured by ELISA kites. (C) **6d** dose dependently induced expression of
389 Nrf2 and its downstream antioxidant proteins in BV2 microglia cells. (D) Nrf2
390 expression in Control siRNA- and Nrf2 siRNA-transfected BV2 microglia cells. (***p)
391 ≤ 0.001 compared with the control group; (^^p) ≤ 0.01 and (^^^p) ≤ 0.001 compared
392 with LPS-treated group. Transfection of BV2 microglia cells with Nrf2 siRNA
393 reversed suppressive effects of **6d** (20 μM) on NO (E), IL-6 (F) production following
394 LPS stimulation. **p≤0.01 and *p≤0.05 in comparison with control siRNA-transfected
395 cells. Data are presented by mean ± SD (n = 3).

396 ***2.6 Molecular docking study between 6d and Keap1***

397 Keap1 has strict regulation on the activation of Nrf2. The oxidative or
398 electrophilic agents covalently bind to the cysteine-rich Keap1 protein, thereby
399 changing conformational of Keap1 to prevent the ubiquitination of Nrf2, thus activate
400 Keap1-Nrf2-ARE pathway. According to previous reports, other Michael receptors
401 may activate the Nrf2 pathway by reacting with CYS151 or other reactive cysteine
402 residues in Keap1 [4, 52]. Considering that α, β-unsaturated ketone of **6d** is a Michael
403 receptor moiety, which is possible to react with cysteine residues of keap1. So the
404 covalently docking study was performed used Glide based on the X-ray crystal
405 structure of BTB domain of KEAP1 in complex with CDDO (PDB: 4CXT) (**Figure**
406 **11**). The result of covalent docking showed that **6d** could covalently bonding with
407 CYS151 of Keap1, the benzene ring formed π-π stacking with residue HIE154, and the
408 carbonyl group of α, β-unsaturated ketone and carbonyl lactam formed hydrogen bonds
409 with residues GLY148, LYS131 and ARG135. The *N*-ethyl, *N*-methylformamide

fragment formed hydrogen bonds with LYS150. The above results suggested that **6d** may covalently bind to Keap1, triggered the release of Nrf2 from Keap1, and further promoted Nrf2 translocate into nucleus, where it binded to the ARE to initiate the expression of Nrf2-dependent genes and proteins.

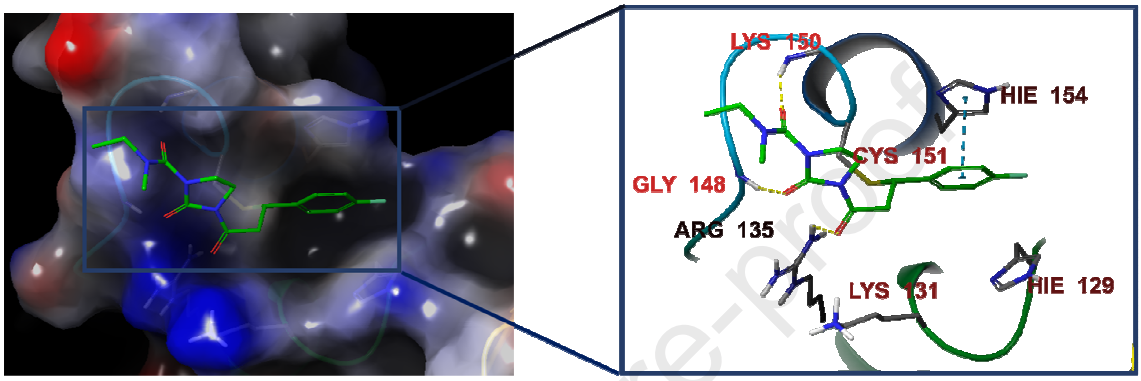

Figure 11. The docking model of **6d** with representative CYS in Keap1. 3D image of covalent docking between **6d** and CYS151 in the BTB domain (PDB: 4CXT).

2.7 In vitro blood-brain barrier (BBB) permeation assay

Favorable blood-brain barrier (BBB) permeability is essential property for a central nervous system (CNS) drug. To verify whether **6d** can penetrate the blood-brain barrier, PAMPA-BBB assay was used. This method is a fast and efficient method to evaluate the BBB permeability, established by Di *et al*, and is widely used in the initial screening of drugs [53]. Eight clinical drugs with different blood-brain barrier permeability were selected to set up the model (**Table 4**). A plot of experimental data versus bibliographic values gave a good linear correlation, Pe (exp.) = 1.080Pe (bibl.) + 1.046 (R^2 = 0.9885) (**Figure S5**). According to this equation and considering the limit established by Di et al. for BBB permeation, it was concluded that compounds with Pe > 5.36×10^{-6} cm s^{-1} can be considered to show good BBB permeation (CNS +).

Journal Pre-proof

Based on the measured permeability (Pe = (6.78 ± 0.3) × 10^{-6} cm s^{-1} cm / s), **6d** could cross the BBB.

3. Conclusion

In conclusion, a series of novel Piperlongumine analogues as antioxidant and anti-inflammatory agents was designed and synthesized. Among these analogues, **6d** exhibited the most potent protective effect against 6-OHDA- or H_2O_2- induced PC12 cell damage. The biological evaluation showed that **6d** is a neuroprotective compound via alleviation or neutralization of ROS accumulation, mitochondrial dysfunction, cell apoptosis and reduces Ca^{2+} overload. Notably, **6d** could reduce the production of NO and IL-6 in LPS-stimulated BV2 microglia cells, indicating its potential anti-inflammatory activity. ROS scavenging and cytoprotection effect of **6d** was implemented by activating Nrf2 and upregulating related phase II antioxidant enzymes, such as HO-1, NQO1, GCLM, GCLC, and TrxR1. We also checked the nuclear and cytoplasmic expression of Nrf2, these results indicated that **6d** promoted the transfer of Nrf2 to the nucleus. Interestingly, the protective effect of **6d** could be significantly weakened by Nrf2 inhibitor brusatol or HO-1 inhibitor ZnPP at non-toxic concentrations, confirming that the antioxidant and anti-inflammatory activity of **6d** is related to the activation of Nrf2. The result of the parallel artificial membrane permeability assay indicated that **6d** would be inclined to cross the BBB. These results, together with the relative safety profile, indicated that **6d** is promising for further development as a therapeutic drug against oxidative stress- and inflammation-related neurodegenerative disorders.

Journal Pre-proof

4. Experimental section

4.1. Chemistry

All conventional reagents and solvents are purchased directly from commercial companies and no further purification is required. Analytical thin-layer chromatography was used to monitor the progress of the reaction on a pre-coated silica gel GF254 plate (Qingdao Haiyang Chemical Plant, Qingdao, China), and to detect spots under ultraviolet light (254 nm). After the reaction is worked up, the product is isolated by rapid purification preparative liquid chromatography (Biotage, Isolera One, Sweden). The melting point was measured with an XT-4 micro-melting point instrument without correction. The ^{1}H NMR and ^{13}C NMR spectra were measured at 25 °C with a Bruker ACF-500 / 600 spectrometer, and reference was made to TMS. The residual solvent line is designated as the internal standard, the chemical shift is expressed in ppm (δ), and the split mode is designed as s, singlet; d, doublet; t, triplet; m, multiplet. An Agilent 6520B Q-TOF mass spectrometer (Agilent Technologies, Santa Clara, California, USA) was used for high-resolution electrospray ionization (HRESI) mass spectrometry.

4.2 Preparation

4.2.1 Preparation of compounds ***PL-1~PL-6*** and *compounds* ***1-5***

The starting material, 5, 6-dihydro-1*H*-pyridin-2-one, 2-piperidone, propyleneurea, 2-imidazolidone and 2-piperazinone (1 equiv.) was added to tetrahydrofuran or dichloromethane under nitrogen, and added NaH (3 equiv.) to the reaction mixture at 0 °C for 15 minutes. Then, (+) - cinnamyl chloride (1 equiv.) was added to the mixture

Journal Pre-proof

with stirring at 20 °C for 30 min. The reaction was quenched with saturated $NaHCO_3$ solution, and then extracted twice with ethyl acetate. The combined extracts were then washed successively with H_2O, brine, and dried over anhydrous Na_2SO_4. After concentration under reduced pressure, the residue was quickly purified by using a flash silica gel column (PE / EtOAc).

*1-cinnamoyl-5,6-dihydropyridin-2(1H)-one (**PL-1**)*

Yield 64%, white powder. m.p. 95-97 °C. ^{1}H NMR (500 MHz, $CDCl_3$) δ 7.75 (d, J = 15.7 Hz, 1H), 7.58 (dd, J = 5.2, 2.0 Hz, 2H), 7.52 (d, J = 15.5 Hz, 1H), 7.37 (dd, J = 5.2, 2.0 Hz, 3H), 6.93 (dt, J = 9.7, 4.2 Hz, 1H), 6.05 (dt, J = 9.8, 1.9 Hz, 1H), 4.04 (t, J = 6.5 Hz, 2H), 2.48 (m, J = 6.3, 4.1, 1.9 Hz, 2H).^{13}C NMR (125 MHz, $CDCl_3$) δ 168.95, 165.77, 145.38, 143.61, 135.15, 130.02, 128.77, 128.34, 125.90, 121.91, 41.62, 24.83. HRMS (ESI) *m/z* 250.0840 $[M+Na]^+$ (calcd for 250.0838, $C_{14}H_{13}NNaO_2$).

*1-cinnamoylpiperidin-2-one (**PL-2**)*

Yield 94%, white powder. m.p. 85-87° C. ^{1}H NMR (600 MHz, $CDCl_3$) δ 7.71 (d, J = 15.6 Hz, 1H), 7.59 - 7.55 (m, 2H), 7.45 (d, J = 15.6 Hz, 1H), 7.37 (dd, J = 5.1, 2.1 Hz, 3H), 3.80 (td, J = 5.3, 4.4, 2.0 Hz, 2H), 2.61 (td, J = 6.1, 5.0, 3.7 Hz, 2H), 1.91 – 1.87 (m, 4H). ^{13}C NMR (150 MHz, $CDCl_3$) δ 173.88, 169.76, 143.20, 135.05, 129.98, 128.74, 128.28, 122.06, 44.64, 34.95, 22.57, 20.65. HRMS (ESI) *m/z* 230.1169 $[M+H]^+$ (calcd for 230.1176, $C_{14}H_{16}NO_2$).

1-cinnamoyltetrahydropyrimidin-2(1*H*)-one (***PL-3***)

Yield 25%, yellow powder. m.p. 189-191 °C. ^{1}H NMR (500 MHz, $CDCl_3$) δ 7.80 (d, J = 15.7 Hz, 1H), 7.74 (d, J = 15.7 Hz, 1H), 7.62 (dd, J = 7.2, 2.0 Hz, 2H), 7.40 (d,

Journal Pre-proof

495 *J* = 6.6 Hz, 3H), 3.96 - 3.91 (m, 2H), 3.43 (t, *J* = 5.6 Hz, 2H), 2.06 (p, *J* = 6.0 Hz, 2H).
496 ^{13}C NMR (125 MHz, $CDCl_3$) δ 168.57, 142.79, 135.38, 129.75, 128.93, 128.69, 128.26,
497 122.13, 41.92, 40.78, 21.84. HRMS (ESI) *m/z* 231.1125 $[M+H]^+$ (calcd for 231.1128 ,
498 $C_{13}H_{15}N_2O_2$).
499 1-cinnamoylimidazolidin-2-one (***PL-4***)
500 Yield 84%, white powder. m.p. 205-207 °C. ^{1}H NMR (600 MHz, $CDCl_3$) δ 8.03
501 (d, *J* = 15.8 Hz, 1H), 7.82 (d, *J* = 15.8 Hz, 1H), 7.65 - 7.60 (m, 2H), 7.38 (dd, *J* = 4.9,
502 2.4 Hz, 3H), 5.02 (s, 1H), 4.08 (dd, *J* = 8.6, 7.3 Hz, 2H), 3.59 - 3.52 (m, 2H). ^{13}C NMR
503 (150 MHz, $CDCl_3$) δ 165.95, 156.81, 144.22, 135.09, 130.11, 128.76, 128.45, 118.35,
504 42.65, 36.63. HRMS (ESI) *m/z* 217.0965 $[M+H]^+$ (calcd for 217.0972, $C_{14}H_{16}NO_2$).
505 4-cinnamoylpiperazin-2-one (***PL-5***)
506 Yield 14%, yellow powder. m.p. 140-142 °C. ^{1}H NMR (500 MHz, $CDCl_3$) δ 7.74
507 (d, *J* = 15.3 Hz, 1H), 7.57 - 7.51 (m, 2H), 7.39 (dd, *J* = 5.2, 2.0 Hz, 3H), 6.81 (d, *J* =
508 15.3 Hz, 1H), 4.35 (s, 2H), 3.91 (s, 2H), 3.47 (d, *J* = 6.2 Hz, 2H). ^{13}C NMR (125 MHz,
509 $CDCl_3$) δ 165.39, 144.31, 134.79, 130.10, 128.91, 127.94, 115.91, 48.97, 40.74, 38.83.
510 HRMS (ESI) *m/z* 231.1123 $[M+H]^+$ (calcd for 231.1128 , $C_{13}H_{15}N_2O_2$).
511 1- (3-phenylpropanoyl) imidazolidin-2-one (***PL-6***)
512 Yield 58%, yellow powder. m.p. 121-122 °C. ^{1}H NMR (500 MHz, DMSO-d_6) δ
513 7.56 (s, 1H), 7.28 (t, *J* = 7.4 Hz, 2H), 7.23 (d, *J* = 7.1 Hz, 2H), 7.18 (t, *J* = 7.2 Hz, 1H),
514 3.78 - 3.72 (m, 2H), 3.32 (s, 2H), 3.11 (t, *J* = 7.8 Hz, 2H), 2.84 (t, *J* = 7.8 Hz, 2H). ^{13}C
515 NMR (125 MHz, DMSO-d_6) δ 172.18, 156.48, 141.75, 128.76, 128.73, 126.32, 42.31,

36.81, 36.23, 30.66. HRMS (ESI) *m/z* 241.0945 $[M+Na]^+$ (calcd for 241.0947, $C_{12}H_{14}N_2NaO_2$).

*4.2.2 General procedures for the preparation of (**1-5**)*

Concentrated 2-Imidazolidone (1 equiv.) were added to absolute dichloromethane under nitrogen, and added NaH (3 equiv.) to the reaction mixture was stirred at 0 ^oC for 15 minutes and then added to (+)-cinnamyl chloride with different substituents (1 equiv.) to the reaction mixture was stirred at 20 ^oC for 30 min. After the reaction was completed, it was quenched with saturated $NaHCO_3$ solution, and then the mixed liquid was extracted twice with ethyl acetate. The combined extracts were then washed with H_2O and brine, and dried over anhydrous Na_2SO_4. After concentration under reduced pressure, the residue was quickly purified by using a silica gel column (PE / EtOAc).

(*E*)-1-(3-(4- (trifluoromethyl) phenyl) acryloyl) imidazolidin-2-one (***1***)

Yield 63%, white powder. m.p. 195-197 °C. ^1H NMR (500 MHz, $CDCl_3$) δ 8.00 (d, J = 15.7 Hz, 1H), 7.82 (d, J = 15.7 Hz, 1H), 7.64 (dd, J = 8.3, 5.4 Hz, 2H), 7.11 (t, J = 8.3 Hz, 2H), 5.35 (s, 1H), 4.12 (t, J = 7.9 Hz, 2H), 3.60 (t, J = 7.9 Hz, 2H). ^{13}C NMR (125 MHz, $CDCl_3$) δ 165.82, 163.87(d, $J_{c\text{-}f}$ = 249.5 Hz), 156.68, 142.93, 131.35, 130.36, 118.07, 115.90 (d, $J_{c\text{-}f}$ = 21.25 Hz), 42.66, 36.62. HRMS (ESI) m/z 235.0871 $[M+H]^+$ (calcd for 235.0877, $C_{12}H_{12}FN_2O_2$).

(*E*)-1-(3-(thiophen-2-yl) acryloyl) imidazolidin-2-one (***2***)

Yield 54%, white powder. m.p. 128-129 °C. ^1H NMR (600 MHz, $CDCl_3$) δ 7.85 (d, J = 15.5 Hz, 1H), 7.57 (d, J = 15.5 Hz, 1H), 7.49 (d, J = 1.7 Hz, 1H), 6.65 (d, J =

Journal Pre-proof

538 3.4 Hz, 1H), 6.46 (dd, *J* = 3.4, 1.8 Hz, 1H), 5.35 (s, 1H), 4.06 (dd, *J* = 8.6, 7.3 Hz, 2H),
539 3.54 (ddd, *J* = 8.7, 7.4, 0.9 Hz, 2H). ^{13}C NMR (150 MHz, $CDCl_3$) δ 165.83, 156.70,
540 151.69, 144.64, 130.56, 115.84, 114.92, 112.25, 42.64, 36.61. HRMS (ESI) *m/z*
541 245.0351 $[M+Na]^+$ (calcd for 245.0355, $C_{10}H_{10}N_2NaO_2S$).

542 (*E*)-1-(3-(furan-2-yl) acryloyl) imidazolidin-2-one (***3***)

543 Yield 28%, yellow powder. m.p. 198-200 °C. ^{1}H NMR (600 MHz, $CDCl_3$) δ 7.87
544 (d, *J* = 15.5 Hz, 1H), 7.59 (d, *J* = 15.5 Hz, 1H), 7.51 (d, *J* = 1.4 Hz, 1H), 6.67 (d, *J* =
545 3.4 Hz, 1H), 6.48 (dd, *J* = 3.4, 1.8 Hz, 1H), 5.37 (s, 1H), 4.10 – 4.06 (m, 2H), 3.56 (t, *J*
546 = 8.0 Hz, 2H). ^{13}C NMR (150 MHz, $CDCl_3$) δ 165.84, 156.72, 151.70, 144.66, 130.57,
547 115.85, 114.93, 112.26, 42.65, 36.62. HRMS (ESI) *m/z* 229.0576 $[M+Na]^+$ (calcd for
548 229.0584, $C_{10}H_{10}N_2NaO_3$).

549 (*E*)-1-(3-(4-(trifluoromethyl) phenyl) acryloyl) imidazolidin-2-one (***4***)

550 Yield 66%, white powder. m.p. 187-189 °C. ^{1}H NMR (500 MHz, $CDCl_3$) δ 8.08
551 (d, *J* = 15.8 Hz, 1H), 7.85 - 7.77 (m, 3H), 7.62 (d, *J* = 7.6 Hz, 1H), 7.51 (t, *J* = 7.6 Hz,
552 1H), 5.35 (s, 1H), 4.09 (t, *J* = 7.8 Hz, 2H), 3.57 (t, *J* = 7.8 Hz, 2H). ^{13}C NMR (125
553 MHz, $CDCl_3$) δ 165.42, 156.55, 142.30, 135.88, 131.29, 129.30, 126.42, 125.02,
554 120.22, 42.63, 36.62. HRMS (ESI) *m/z* 307.0656 $[M+Na]^+$ (calcd for 307.0665,
555 $C_{13}H_{11}F_3N_2NaO_2$).

556 1-(3-(4- fluorophenyl) propanoyl) imidazolidin-2-one (***5***)

557 Yield 56%, white powder. m.p. 121-122 °C. ^{1}H NMR (500 MHz, $CDCl_3$) δ 7.20
558 (dd, *J* = 8.1, 5.7 Hz, 2H), 6.95 (t, *J* = 8.7 Hz, 2H), 5.20 (s 1H), 3.97 - 3.91 (m, 2H),
559 3.48 (t, *J* = 8.0 Hz, 2H), 3.22 (t, *J* = 7.7 Hz, 2H), 2.95 (t, *J* = 7.6 Hz, 2H). ^{13}C NMR

Journal Pre-proof

(125 MHz, $CDCl_3$) δ 172.71, 161.39 (d, $J_{c\text{-}f}$ = 242.13), 129.99, 115.06 (d, $J_{c\text{-}f}$ =21.0), 77.26, 42.30, 37.00, 36.56, 29.78. HRMS (ESI) m/z 259.0851 $[M+Na]^+$(calcd for 259.0853, $C_{12}H_{13}FN_2NaO_2$).

4.2.3 General procedures for the preparation of ***6-29***

Firstly, the cinnamic acid analogues (1 equiv.) with different substituents are added, dropwise stir in triethylamine ice bath for 15 min. then add trimethylacetyl chloride to protect the N-H at one end. After concentration under reduced pressure, the residue was quickly purified by using a silica gel column (PE / EtOAc). Here, do not contact water for reaction and products, and it needs to be quickly purified and concentrated. Concentrated 2-imidazolidone (1 equiv.) were added to absolute tetrahydrofuran or dichloromethane under nitrogen, and added NaH (3 equiv.) to the reaction mixture was stirred at 0 °C for 15 minutes. Then add the above products to the reaction mixture was stirred at 0 °C for 30 min. After the reaction was completed, used quenching with saturated $NaHCO_3$ solution, and then the mixed liquid was extracted twice with ethyl acetate. The combined extracts were then washed with H_2O and brine and dried over anhydrous Na_2SO_4. After concentration under reduced pressure, the residue was quickly purified by using a silica gel column (PE / EtOAc).

(*E*)-1-(3-(4- fluorophenyl) acryloyl)-3-pivaloylimidazolidin-2-one (***6***)

Yield 62%, white powder. m.p. 146-148 °C. ^{1}H NMR (500 MHz, $CDCl_3$) δ 7.87 (d, J = 15.7 Hz, 1H), 7.82 (d, *J* = 15.8 Hz, 1H), 7.63 (dd, J = 8.6, 5.4 Hz, 2H), 7.09 (t, *J* = 8.6 Hz, 2H), 3.97 – 3.91 (m, 2H), 3.90 – 3.86 (m, 2H), 1.41 (s, 9H). ^{13}C NMR (125 MHz, $CDCl_3$) δ 179.51, 166.12, 164.08 (d, $J_{c\text{-}f}$ = 250.13 Hz), 150.82, 144.32, 131.11,

582 130.56, 117.74, 116.04 (d, $J_{c\text{-}f}$ = 21.75 Hz), 41.65, 41.23, 39.31, 26.44. HRMS (ESI)

583 m/z 319.1445 $[M+H]^+$ (calcd for 319.1452, $C_{19}H_{20}FN_2O_3$).

584 (*E*)-1-(3-(4-nitrophenyl)acryloyl)-3-pivaloylimidazolidin-2-one（***7***）

585 Yield 64%, yellow powder. m.p. 196-197 °C. ^{1}H NMR (500 MHz, $CDCl_3$) δ 8.26

586 (d, *J* = 8.7 Hz, 2H), 8.05 (d, *J* = 15.8 Hz, 1H), 7.86 (d, *J* = 15.8 Hz, 1H), 7.77 (d, *J* =

587 8.7 Hz, 2H), 3.96 (ddd, *J* = 9.3, 6.1, 2.2 Hz, 2H), 3.90 (ddd, *J* = 9.8, 6.0, 2.2 Hz, 2H),

588 1.42 (s, 9H). ^{13}C NMR (125 MHz, $CDCl_3$) δ 179.39, 165.37, 150.77, 148.58, 142.24,

589 140.88, 129.09, 124.14, 122.20, 41.67, 41.27, 39.29, 26.38. HRMS (ESI) *m/z* 368.1206

590 $[M+Na]^+$ (calcd for 368.1217, $C_{17}H_{19}N_3NaO_5$).

591 (*E*)-1-(3-(4-chlorophenyl) acryloyl)-3-pivaloylimidazolidin-2-one (***8***)

592 Yield 48%, white powder. m.p. 155-157 °C. ^{1}H NMR (600 MHz, $CDCl_3$) δ 7.91

593 (d, *J* = 15.8 Hz, 1H), 7.81 (d, *J* = 15.7 Hz, 1H), 7.57 (d, *J* = 8.5 Hz, 2H), 7.38 (d, *J* =

594 8.5 Hz, 2H), 3.94 (ddd, *J* = 8.9, 6.2, 1.5 Hz, 2H), 3.88 (ddd, *J* = 9.3, 6.2, 1.5 Hz, 2H),

595 1.41 (s, 9H). ^{13}C NMR (150 MHz, $CDCl_3$) δ 179.48, 166.00, 150.78, 144.11, 136.40,

596 133.29, 129.75, 129.15, 118.51, 41.64, 41.22, 39.29, 26.41. HRMS (ESI) *m/z* 335.1146

597 $[M+H]^+$(calcd for 335.1157, $C_{17}H_{20}ClN_2O_3$).

598 (*E*)-1-(3-(4-bromophenyl) acryloyl)-3-pivaloylimidazolidin-2-one (***9***)

599 Yield 62%, white powder. m.p. 178-180 °C. ^{1}H NMR (500 MHz, $CDCl_3$) δ 7.92

600 (d, *J* = 15.7 Hz, 1H), 7.79 (d, *J* = 15.7 Hz, 1H), 7.57 - 7.46 (m, 4H), 3.97 - 3.91 (m,

601 2H), 3.91 - 3.84 (m, 2H), 1.41 (s, 9H). ^{13}C NMR (125 MHz, $CDCl_3$) δ 179.00, 165.51,

602 150.31, 143.70, 133.24, 131.64, 129.48, 124.30, 118.14, 41.17, 40.75, 38.81, 25.94.

603 HRMS (ESI) *m/z* 401.0461 $[M+Na]^+$(calcd for 401.0471, $C_{17}H_{19}BrN_2NaO_3$).

Journal Pre-proof

Journal Pre-proof

(*E*)-1-pivaloyl-3-(3-(3,4,5-trimethoxyphenyl) acryloyl) imidazolidin-2-one (***10***)

Yield 45%, white powder. m.p. 114-116 °C. ^{1}H NMR (500 MHz, $CDCl_3$) δ 7.78 (s, 2H), 6.85 (s, 2H), 3.92 (s, 8H), 3.88 (d, J = 8.4 Hz, 5H), 1.41 (s, 9H). ^{13}C NMR (125 MHz, $CDCl_3$) δ 179.48, 166.14, 153.40, 150.77, 145.67, 140.50, 130.31, 117.20, 105.96, 60.95, 56.30, 41.60, 41.24, 39.33, 26.43. HRMS (ESI) *m/z* 391.1858 $[M+H]^+$ (calcd for 391.1864, $C_{20}H_{27}N_2O_6$).

(*E*)-1-(3-(4-methoxyphenyl) acryloyl)-3-pivaloylimidazolidin-2-one (***11***)

Yield 56%, white powder. m.p. 148-150 °C. ^{1}H NMR (500 MHz, $CDCl_3$) δ 7.85 (d, J = 15.7 Hz, 1H), 7.80 (d, J = 15.7 Hz, 1H), 7.60 (d, J = 8.8 Hz, 2H), 6.92 (d, J = 8.8 Hz, 2H), 3.95 - 3.91 (m, 2H), 3.89 - 3.85 (m, 2H), 3.85 (s, 3H), 1.42 (s, 9H). ^{13}C NMR (125 MHz, $CDCl_3$) δ 179.54, 166.47, 161.64, 150.82, 145.50, 130.37, 127.63, 115.45, 114.31, 55.40, 41.62, 41.19, 39.30, 26.44. HRMS (ESI) m/z 353.1465 $[M+Na]^+$ (calcd for 353.1472, $C_{18}H_{22}N_2NaO_4$).

(*E*)-4-(3-oxo-3-(2-oxo-3-pivaloylimidazolidin-1-yl) prop-1-en-1-yl) benzonitrile (***12***)

Yield 72%, white powder. m.p. 193-195 °C. ^{1}H NMR (500 MHz, $CDCl_3$) δ 8.02 (d, J = 15.8 Hz, 1H), 7.81 (d, J = 15.8 Hz, 1H), 7.73 - 7.68 (m, 4H), 3.95 (ddd, J = 9.3, 6.1, 2.2 Hz, 2H), 3.90 (ddd, J = 9.7, 6.1, 2.2 Hz, 2H), 1.41 (s, 9H). ^{13}C (125 MHz, $CDCl_3$) δ 179.41, 165.48, 150.78, 142.82, 139.07, 128.85, 121.51, 118.43, 113.50, 41.68, 41.27, 39.30, 26.40. HRMS (ESI) *m/z* 348.1314 $[M+Na]^+$ (calcd for 348.1319, $C_{18}H_{19}N_3NaO_3$).

(*E*)-1-(3-(3- fluorophenyl) acryloyl)-3-pivaloylimidazolidin-2-one (**13**)

Yield 68%, white powder. m.p. 167-169 °C. ^{1}H NMR (500 MHz, $CDCl_3$) δ 7.94

626 (d, *J* = 15.7 Hz, 1H), 7.82 (d, *J* = 15.7 Hz, 1H), 7.42 – 7.33 (m, 3H), 7.11 (t, *J* = 7.8 Hz,
627 1H), 3.95 (dd, *J* = 8.3, 5.5 Hz, 2H), 3.92 – 3.88 (m, 2H), 1.43 (s, 9H). ^{13}C NMR (126
628 MHz, $CDCl_3$) δ 179.47, 165.88, 163.03 (d, $J_{c\text{-}f}$ = 245.0Hz), 150.74, 144.05, 137.07,
629 130.42, 124.59, 119.38, 117.36 (d, $J_{c\text{-}f}$ = 29.13Hz), 114.70 (d, $J_{c\text{-}f}$ = 21.75Hz), 41.63,
630 41.21, 39.26, 26.40. HRMS (ESI) *m/z* 319.1445 $[M+H]^+$ (calcd for 319.1452,
631 $C_{17}H_{20}FN_2O_3$).

632 (*E*)-1-(3-(2-fluorophenyl) acryloyl)-3-pivaloylimidazolidin-2-one (***14***)

633 Yield 61%, white powder. m.p. 160-162 °C. ^{1}H NMR (500 MHz, $CDCl_3$) δ 8.27
634 (d, *J* = 15.7 Hz, 1H), 7.91 (d, *J* = 15.7 Hz, 1H), 7.79 - 7.76 (m, 1H), 7.44 - 7.40 (m,
635 1H), 7.34 - 7.28 (m, 2H), 3.97 - 3.93 (m, 2H), 3.91 - 3.86 (m, 2H), 1.41 (s, 9H). ^{13}C
636 NMR (125 MHz, $CDCl_3$) δ 179.48, 165.79, 150.79, 141.24, 135.36, 133.11, 131.18,
637 130.13, 128.13, 127.06, 120.52, 41.63, 41.25, 39.29, 26.41. HRMS (ESI) *m/z* 319.1445
638 $[M+H]^+$ (calcd for 319.1452, $C_{17}H_{20}FN_2O_3$).

639 (*E*)-1-pivaloyl-3-(3-(4-(trifluoromethyl) phenyl) acryloyl) imidazolidin-2-one (***15***)

640 Yield 38%, white powder. m.p. 114-116 °C. ^{1}H NMR (600 MHz, $CDCl_3$) δ 8.00
641 (d, *J* = 15.8 Hz, 1H), 7.89 (d, *J* = 15.8 Hz, 1H), 7.85 (d, *J* = 5.7 Hz, 2H), 7.67 (d, *J* =
642 7.8 Hz, 1H), 7.56 (t, *J* = 7.8 Hz, 1H), 3.99 - 3.95 (m, 2H), 3.94 - 3.90 (m, 2H), 1.44 (s,
643 9H). ^{13}C NMR (150 MHz, $CDCl_3$) δ 179.49, 165.77, 150.74, 143.68, 135.54, 131.52,
644 129.42, 126.85, 125.31, 119.83, 41.66, 41.25, 39.30, 26.40. HRMS (ESI) *m/z* 391.1238
645 $[M+Na]^+$ (calcd for 391.1240, $C_{18}H_{19}F_3N_2NaO_3$).

646 (*E*)-1-(3-(4-bromo-2-fluorophenyl) acryloyl)-3-pivaloylimidazolidin-2-one (***16***)

Journal Pre-proof

Journal Pre-proof

Yield 66%, white powder. m.p. 110-112 °C. ^{1}H NMR (500 MHz, $CDCl_3$) δ 8.15 (d, J = 15.7 Hz, 1H), 7.82 (d, J = 15.6 Hz, 1H), 7.76 (t, J = 7.1 Hz, 1H), 7.37 (d, J = 7.9 Hz, 1H), 7.09 (t, J = 8.2 Hz, 1H), 3.97 - 3.92 (m, 2H), 3.89 (dt, J = 9.3, 4.4 Hz, 2H), 1.41 (s, 9H). ^{13}C NMR (125 MHz, $CDCl_3$) δ 179.45, 165.57, 164.21, 162.21, 150.83, 142.57, 131.28, 129.56 (d, $J_{c\text{-}f}$ = 8.88 Hz), 126.12, 120.73, 120.53, 115.31 (d, $J_{c\text{-}f}$ = 21.38 Hz), 41.65, 41.27, 39.30, 26.42. HRMS (ESI) *m/z* 419.0366 $[M+Na]^+$ (calcd for 419.0377, $C_{17}H_{18}BrFN_2NaO_3$).

(*E*)-1-(3-(2-chlorophenyl) acryloyl)-3-pivaloylimidazolidin-2-one (***17***)

Yield 49%, white powder. m.p. 162-164 °C. ^{1}H NMR (600 MHz, $CDCl_3$) δ 7.94 (d, J = 15.7 Hz, 1H), 7.80 (d, J = 15.7 Hz, 1H), 7.63 (s, 1H), 7.52 (d, J = 7.3 Hz, 1H), 7.41 - 7.34 (m, 2H), 4.00 - 3.94 (m, 2H), 3.93 - 3.87 (m, 2H), 1.44 (s, 9H). ^{13}C NMR (125 MHz, $CDCl_3$) δ 179.47, 165.78, 150.79, 141.24, 135.36, 133.11, 131.18, 130.13, 128.12, 127.06, 120.51, 41.25, 39.29, 26.41. HRMS (ESI) *m/z* 335.1152 $[M+H]^+$ (calcd for 335.1157, $C_{17}H_{20}ClN_2O_3$).

(*E*)-1-(3-(3-chlorophenyl) acryloyl)-3-pivaloylimidazolidin-2-one (***18***)

Yield 64%, white powder. m.p. 174-176 °C. ^{1}H NMR (600 MHz, $CDCl_3$) δ 7.94 (d, J = 15.7 Hz, 1H), 7.80 (d, J = 15.7 Hz, 1H), 7.63 (s, 1H), 7.52 (d, J = 7.3 Hz, 1H), 7.41 - 7.34 (m, 2H), 3.99 - 3.89 (m, 4H), 1.44 (s, 9H). ^{13}C NMR (150 MHz, $CDCl_3$) δ 179.49, 165.87, 150.73, 143.92, 136.58, 134.87, 130.35, 130.11, 128.18, 126.81, 119.34, 41.65, 41.22, 39.28, 26.40. HRMS (ESI) *m/z* 335.1152 $[M+H]^+$ (calcd for 335.1157, $C_{17}H_{20}ClN_2O_3$).

(*E*)-1-pivaloyl-3-(3-(p-tolyl) acryloyl) imidazolidin-2-one (***19***)

Journal Pre-proof

669 Yield 52%, white powder. m.p. 170-172 °C. ^{1}H NMR (600 MHz, $CDCl_3$) δ 7.89
670 (d, J = 15.7 Hz, 1H), 7.85 (d, J = 15.7 Hz, 1H), 7.55 - 7.53 (m, 2H), 7.21 (d, J = 7.9 Hz,
671 2H), 3.94 (ddd, J = 9.1, 6.4, 1.4 Hz, 2H), 3.87 (ddd, J = 9.1, 6.4, 1.5 Hz, 2H), 2.39 (s,
672 3H), 1.42 (s, 9H). ^{13}C NMR (150 MHz, $CDCl_3$) δ 179.54, 166.42, 150.77, 145.81,
673 141.04, 132.05, 129.60, 128.65, 116.79, 41.62, 41.20, 39.29, 26.42, 21.57. HRMS (ESI)
674 *m/z* 315.1701 $[M+H]^+$ (calcd for 315.1703, $C_{18}H_{23}N_2O_3$).

675 (*E*)-1-pivaloyl-3-(3-(thiophen-2-yl) acryloyl) imidazolidin-2-one (***20***)

676 Yield 49%, white powder. m.p. 179-181 °C. ^{1}H NMR (500 MHz, $CDCl_3$) δ 7.76
677 (d, J = 15.5 Hz, 1H), 7.62 (d, J = 15.5 Hz, 1H), 7.52 (d, J = 1.6 Hz, 1H), 6.69 (d, J =
678 3.4 Hz, 1H), 6.49 (dd, J = 3.4, 1.8 Hz, 1H), 3.93 (ddd, J = 10.0, 6.6, 2.4 Hz, 2H), 3.89 -
679 3.84 (m, 2H), 1.41 (s, 9H). ^{13}C NMR (125 MHz, $CDCl_3$) δ 179.54, 165.98, 150.68,
680 140.18, 137.96, 131.45, 128.95, 128.16, 116.65, 41.63, 41.20, 39.28, 26.43. HRMS
681 (ESI) *m/z* 291.1332 $[M+H]^+$ (calcd for 291.1339, $C_{15}H_{19}N_2O_4$).

682 (*E*)-1-(3-(furan-2-yl) acryloyl)-3-pivaloylimidazolidin-2-one (***21***)

683 Yield 53%, white powder. m.p. 142-143°C. ^{1}H NMR (500 MHz, $CDCl_3$) δ 7.76 (d,
684 J = 15.5 Hz, 1H), 7.62 (d, J = 15.5 Hz, 1H), 7.52 (d, J = 1.6 Hz, 1H), 6.69 (d, J = 3.4
685 Hz, 1H), 6.49 (dd, J = 3.4, 1.6 Hz, 1H), 3.96 - 3.84 (m, 4H), 1.41 (s, 9H). ^{13}C NMR
686 (125 MHz, $CDCl_3$) δ 179.55, 166.13, 151.52, 150.67, 145.03, 131.72, 115.78, 115.44,
687 112.44, 41.62, 41.19, 39.29, 26.44. HRMS (ESI) *m/z* 307.1106 $[M+H]^+$ (calcd for
688 307.1111, $C_{15}H_{19}N_2O_3S$).

689 1-cinnamoyl-3-pivaloylimidazolidin-2-one (***22***)

Journal Pre-proof

690 Yield 62%, white powder. m.p. 141-143°C. ^{1}H NMR (500 MHz, $CDCl_3$) δ 7.99 (d,
691 J = 15.7 Hz, 1H), 7.92 (d, J = 15.7 Hz, 1H), 7.70 - 7.67 (m, 2H), 7.47 - 7.43 (m, 3H),
692 4.01 - 3.97 (m, 2H), 3.95 - 3.90 (m, 2H), 1.46 (s, 9H). ^{13}C NMR (125 MHz, $CDCl_3$) δ
693 179.54, 166.27, 150.79, 145.68, 134.82, 128.88, 128.62, 118.00, 41.65, 41.23, 39.31,
694 26.45. HRMS (ESI) *m/z* 301.1537 $[M+H]^+$ (calcd for 301.1547, $C_{17}H_{21}N_2O_3$).

695 (*E*)-1-pivaloyl-3-(3-(pyridin-3-yl) acryloyl) imidazolidin-2-one (***23***)

696 Yield 32%, white powder. m.p. 167-179 °C. ^{1}H NMR (500 MHz, $CDCl_3$) δ 8.87
697 (d, J = 2.2 Hz, 1H), 8.67 (dd, J = 4.9, 1.6 Hz, 1H), 8.09 - 8.02 (m, 2H), 7.88 (d, J =
698 15.8 Hz, 1H), 7.42 (dd, J = 7.9, 4.9 Hz, 1H), 4.00 (ddd, J = 9.8, 6.5, 2.4 Hz, 2H), 3.94
699 (ddd, J = 9.6, 6.5, 2.4 Hz, 2H), 1.46 (s, 9H). ^{13}C NMR (125 MHz, $CDCl_3$) δ 179.44,
700 165.53, 150.77, 150.55, 149.70, 141.32, 135.01, 130.85, 123.91, 120.47, 41.66, 41.25,
701 39.27, 26.40. HRMS (ESI) *m/z* 302.1489 $[M+H]^+$ (calcd for 302.1499, $C_{16}H_{20}N_3O_3$).

702 (*E*)-1-(3-(naphthalen-1-yl) acryloyl)-3-pivaloylimidazolidin-2-one (***24***)

703 Yield 63%, white powder. m.p. 165-167 °C. ^{1}H NMR (500 MHz, $CDCl_3$) δ 8.74
704 (d, J = 15.5 Hz, 1H), 8.28 (d, J = 8.4 Hz, 1H), 8.04 (d, J = 15.5 Hz, 1H), 7.93 (dt, J =
705 15.2, 7.4 Hz, 3H), 7.61 (t, J = 7.2 Hz, 1H), 7.55 (q, J = 7.6 Hz, 2H), 4.00 (dd, J = 9.1,
706 5.9 Hz, 2H), 3.92 (dd, J = 9.2, 5.8 Hz, 2H), 1.44 (s, 9H). ^{13}C NMR (125 MHz, $CDCl_3$)
707 δ 179.51, 166.19, 150.80, 142.40, 133.70, 132.03, 131.66, 130.77, 128.73, 126.90,
708 126.19, 125.56, 125.50, 123.42, 120.44, 41.64, 41.25, 39.32, 26.43. HRMS (ESI) *m/z*
709 351.1696 $[M+H]^+$ (calcd for 351.1703, $C_{21}H_{23}N_2O_3$).

710 (*E*)-1-(3-(benzo[d] [1,3] dioxol-5-yl) acryloyl)-3-pivaloylimidazolidin-2-one (***25***)

Journal Pre-proof

Yield 52%, white powder. m.p. 228-230 °C. ^{1}H NMR (600 MHz, $CDCl_3$) δ 7.78 (d, J = 1.4 Hz, 2H), 7.18 (d, J = 1.7 Hz, 1H), 7.10 (dd, J = 8.0, 1.7 Hz, 1H), 6.83 (d, J = 8.0 Hz, 1H), 6.02 (s, 2H), 3.95 - 3.91 (m, 2H), 3.87 (ddd, J = 9.1, 6.2, 1.5 Hz, 2H), 1.41 (s, 9H). ^{13}C NMR (150 MHz, $CDCl_3$) δ 179.53, 166.33, 150.77, 149.84, 148.30, 145.47, 129.29, 125.19, 115.87, 108.53, 106.98, 101.59, 41.61, 41.17, 39.27, 26.40. HRMS (ESI) *m/z* 315.1435 $[M+H]^+$ (calcd for 315.1445, $C_{18}H_{21}N_2O_5$).

(*E*)-1-(3-(2-chloro-6-fluorophenyl) acryloyl)-3-pivaloylimidazolidin-2-one (***26***)

Yield 70%, white powder. m.p. 155-157 °C. ^{1}H NMR (600 MHz, Chloroform-*d*) δ 8.10 (d, J = 16.1 Hz, 1H), 8.02 (d, J = 16.1 Hz, 1H), 7.25 (s, 2H), 7.08 – 7.04 (m, 1H), 3.95 (dd, J = 9.2, 5.7 Hz, 2H), 3.90 – 3.87 (m, 2H), 1.40 (s, 9H). ^{13}C NMR (150 MHz, $CDCl_3$) δ 179.53, 166.19, 162.83, 161.13, 150.61, 136.33, 135.08, 130.81, 130.74, 125.94, 125.03 (d, $J_{c\text{-}f}$ = 15 Hz), 122.13 (d, $J_{c\text{-}f}$ = 2.3 Hz), 114.91 (d, $J_{c\text{-}f}$ = 22.5 Hz), 41.63, 41.26, 39.30, 26.39. HRMS (ESI) *m/z* 353.1060 $[M+H]^+$ (calcd for 353.1063, $C_{17}H_{19}ClFN_2O_3$).

(*E*)-1-(2-methyl-3-phenylacryloyl)-3-pivaloylimidazolidin-2-one (***27***)

Yield 72%, white powder. m.p. 112-114 °C. ^{1}H NMR (500 MHz, $CDCl_3$) δ 7.44 - 7.37 (m, 4H), 7.30 (t, J = 7.2 Hz, 1H), 6.90 (d, J = 1.8 Hz, 1H), 3.94 - 3.90 (m, 2H), 3.90 - 3.86 (m, 2H), 2.18 (d, J = 1.5 Hz, 3H), 1.36 (s, 9H). ^{13}C NMR (125 MHz, $CDCl_3$) δ 179.38, 172.79, 149.99, 135.79, 134.67, 132.61, 129.53, 128.34, 128.02, 41.58, 41.54, 39.69, 26.34, 15.73. HRMS (ESI) *m/z* 315.1698 $[M+H]^+$ (calcd for 315.1703, $C_{18}H_{23}N_2O_3$).

(*Z*)-1-(3-phenyl-2-(prop-1-en-2-ylamino) acryloyl)-3-pivaloylimidazolidin-2-one (***28***)

Journal Pre-proof

Journal Pre-proof

Yield 46%, white powder. m.p. 144-146 °C. ^{1}H NMR (600 MHz, $CDCl_3$) δ 7.47 - 7.40 (m, 5H), 7.35 (t, J = 7.4 Hz, 1H), 6.39 (s, 1H), 3.96 - 3.84 (m, 4H), 2.06 (s, 3H), 1.34 (s, 9H). ^{13}C NMR (150 MHz, $CDCl_3$) δ 179.10, 168.02, 166.38, 149.89, 133.71, 130.13, 129.07, 128.93, 128.70, 121.84, 41.73, 41.44, 39.33, 26.28. HRMS (ESI) *m/z* 380.1573 $[M+Na]^+$ (calcd for 380.1581, $C_{19}H_{23}N_3NaO_4$).

4.2.4 General procedures for the preparation of ***6a-6n***

Concentrated (*E*)-1-(3-(4-fluorophenyl)acryloyl)imidazolidin-2-one (1 equiv.) were added to absolute dichloromethane under nitrogen, and added NaH (3 equiv.) to the reaction mixture was stirred at 0 ^{o}C for 15 minute and then added to small molecule acid chloride(1 equiv.) to the reaction mixture was stirred at 20 ^{o}C for 30 min. After the reaction was completed, used quenching with saturated $NaHCO_3$ solution, and then the mixed liquid was extracted twice with ethyl acetate. The combined extracts were then washed with H_2O and brine, and dried over anhydrous Na_2SO_4. After concentration under reduced pressure, the residue was quickly purified by using a silica gel column (PE / EtOAc).

(*E*)-1-(3-(4-fluorophenyl) acryloyl)-3-methacryloylimidazolidin-2-one (***6a***)

Yield 22%, white powder. m.p. 165-167 °C. ^{1}H NMR (600 MHz, $CDCl_3$) δ 7.86 (d, J = 16.2 Hz, 1H), δ 7.83 (d, J = 16.2 Hz, 1H), 7.65 - 7.61 (m, 2H), 7.09 (t, J = 8.6 Hz, 2H), 5.47 - 5.46 (m, 1H), 5.42 (s, 1H), 4.04 - 4.01 (m, 2H), 3.94 - 3.91 (m, 2H), 2.12 - 2.09 (m, 3H). ^{13}C NMR (150 MHz, $CDCl_3$) δ 171.46, 164.13(d, $J_{c\text{-}f}$ = 250.35 Hz), 163.29, 151.22, 144.78, 140.43, 130.56, 119.75, 117.35, 116.02 (d, $J_{c\text{-}f}$ = 21.9 Hz),

Journal Pre-proof

754 39.41, 19.37. HRMS (ESI) *m/z* 325.0950 $[M+Na]^+$ (calcd for 325.0959,
755 $C_{16}H_{15}FN_2NaO_3$).

756 (*E*)-1-acryloyl-3-(3-(4-fluorophenyl) acryloyl) imidazolidin-2-one **(*6b*)**

757 Yield 29%, white powder. m.p. 149-150 °C. ^{1}H NMR (500 MHz, $CDCl_3$) δ 7.84
758 (s, 2H), 7.65 – 7.59 (m, 2H), 7.51 (dd, *J* = 17.0, 10.5 Hz, 1H), 7.09 (t, *J* = 8.6 Hz, 2H),
759 6.57 (dd, *J* = 17.0, 1.7 Hz, 1H), 5.91 (dd, *J* = 10.4, 1.8 Hz, 1H), 4.01 - 3.97 (m, 2H),
760 3.97 - 3.93 (m, 2H). ^{13}C NMR (125 MHz, $CDCl_3$) δ 165.88, 165.78, 164.16 (d, $J_{c\text{-f}}$ =
761 250.5 Hz), 151.89, 144.66, 131.30, 130.96, 130.47, 128.11, 117.50, 116.10 (d, $J_{c\text{-f}}$ =
762 21.9 Hz), 39.17, 38.94. HRMS (ESI) *m/z* 311.0791 $[M+Na]^+$ (calcd for 311.0802,
763 $C_{15}H_{13}FN_2NaO_3$).

764 (*E*)-3-(3-(4-fluorophenyl) acryloyl)-N, N-dimethyl-2-oxoimidazolidine-1-carboxamide
765 (***6c***)

766 Yield 24%, yellow powder. m.p. 135-137 °C. ^{1}H NMR (500 MHz, $CDCl_3$) δ 7.87
767 (d, *J* = 15.7 Hz, 1H), 7.80 (d, *J* = 15.8 Hz, 1H), 7.60 (dd, *J* = 8.6, 5.4 Hz, 2H), 7.07 (t, *J*
768 = 8.6 Hz, 2H), 3.98 (t, *J* = 7.8 Hz, 2H), 3.81 (t, *J* = 7.7 Hz, 2H), 3.06 (s, 6H). ^{13}C NMR
769 (125 MHz, $CDCl_3$) δ 166.72, 165.58, 164.26 (d, $J_{c\text{-f}}$ = 250.75 Hz), 151.73, 145.19,
770 130.82, 130.55, 117.00, 116.17(d, $J_{c\text{-f}}$ = 21.88 Hz), 43.94, 39.57, 39.01. HRMS (ESI)
771 *m/z* 306.1244 $[M+H]^+$ (calcd for 306.1248, $C_{15}H_{17}FN_3O_3$).

772 (*E*)-N-ethyl-3-(3-(4-fluorophenyl)acryloyl)-N-methyl-2-oxoimidazolidine-1-carboxami
773 de (***6d***)

774 Yield 16%, white powder. m.p. 108-109 °C. ^{1}H NMR (600 MHz, DMSO-d6) δ
775 7.84 (d, *J* = 15.9 Hz, 1H), 7.73 (q, *J* = 8.4, 7.6 Hz, 3H), 7.29 (t, *J* = 8.8 Hz, 2H), 3.86 (t,

Journal Pre-proof

776 *J* = 7.7 Hz, 2H), 3.67 (t, *J* = 7.7 Hz, 2H), 3.38 – 3.34 (m, 2H), 2.95 (s, 3H), 1.12 (t, *J* =
777 7.1 Hz, 3H). ^{13}C NMR (125 MHz, $CDCl_3$) δ 165.70, 164.025 (d, $J_{c\text{-f}}$ = 249.88 Hz),
778 153.75, 152.40, 143.97, 131.11, 130.47, 117.73, 115.99 (d, $J_{c\text{-f}}$ = 22.5 Hz), 40.71,
779 40.12, 31.47, 30.23, 29.35. HRMS (ESI) m/z 320.1400 $[M+H]^+$ (calcd for 320.1405,
780 $C_{16}H_{19}FN_3O_3$).
781 (*E*)-1-(3-(4-fluorophenyl) acryloyl)-3-(piperidine-1-carbonyl) imidazolidin-2-one (***6e***)
782 Yield 21%, white powder. m.p. 108-109 °C. ^{1}H NMR (600 MHz, $CDCl_3$) δ 7.88
783 (dd, *J* = 15.8, 1.6 Hz, 1H), 7.82 (dd, *J* = 15.8, 1.6 Hz, 1H), 7.63 (dd, *J* = 7.2, 2.1 Hz,
784 2H), 7.09 (td, *J* = 8.5, 1.7 Hz, 2H), 3.99 (t, *J* = 8.1 Hz, 2H), 3.85 (d, *J* = 8.0 Hz, 2H),
785 3.53 (s, 4H), 1.68 (s, 6H). ^{13}C NMR (150 MHz, $CDCl_3$) δ 165.72, 163.99 (d, $J_{c\text{-f}}$
786 =249.9 Hz), 152.79, 152.31, 143.96, 131.07, 130.47, 117.71, 115.98 (d, $J_{c\text{-f}}$ = 22.5 Hz),
787 40.73, 40.02, 31.45, 30.20, 24.31. HRMS (ESI) *m/z* 346.1554 $[M+H]^+$ (calcd for
788 346.1561, $C_{18}H_{21}FN_3O_3$).
789 (*E*)-1-acetyl-3-(3-(4-fluorophenyl) acryloyl) imidazolidin-2-one (***6f***)
790 Yield 19%, white powder. m.p. 204-205 °C. ^{1}H NMR (500 MHz, $CDCl_3$) δ 7.85
791 (s, 2H), 7.64 (dd, *J* = 8.6, 5.5 Hz, 2H), 7.11 (t, *J* = 8.6 Hz, 2H), 3.97 (dd, *J* = 9.3, 5.5
792 Hz, 2H), 3.90 (dd, *J* = 9.3, 5.5 Hz, 2H), 2.59 (s, 3H). ^{13}C NMR (126 MHz, $CDCl_3$) δ
793 170.81, 165.85, 164.12 (d, $J_{c\text{-f}}$ =250.35 Hz), 152.01, 144.55, 130.96, 130.44, 117.42,
794 116.07 (d, $J_{c\text{-f}}$ =21.75 Hz), 38.99, 38.66, 24.14. HRMS (ESI) *m/z* 299.0792 $[M+Na]^+$
795 (calcd for 299.0802, $C_{14}H_{13}FN_2NaO_3$).
796 (*E*)-1-(3-(4-fluorophenyl) acryloyl)-3-propionylimidazolidin-2-one (***6g***)

Journal Pre-proof

Yield 32%, white powder. m.p. 163-164 °C. ^{1}H NMR (500 MHz, $CDCl_3$) δ 7.86 (d, J = 2.1 Hz, 2H), 7.64 (dd, J = 8.5, 5.5 Hz, 2H), 7.11 (t, J = 8.6 Hz, 2H), 4.00 – 3.94 (m, 2H), 3.93 – 3.88 (m, 2H), 3.00 (q, J = 7.3 Hz, 2H), 1.23 (t, J = 7.3 Hz, 3H). ^{13}C NMR (125 MHz, $CDCl_3$) δ 174.69, 165.88, 164.10 (d, $J_{c\text{-f}}$ =250.25 Hz), 151.94, 144.44, 130.96, 130.43, 117.51, 116.05 (d, $J_{c\text{-f}}$ =21.75 Hz), 39.10, 38.78, 29.74, 8.42. HRMS (ESI) *m/z* 313.0949 $[M+Na]^+$ (calcd for 313.0959 , $C_{15}H_{15}FN_2NaO_3$).

(*E*)-1-butyryl-3-(3-(4-fluorophenyl) acryloyl) imidazolidin-2-one (***6h***)

Yield 29%, white powder. m.p. 131-132 °C. ^{1}H NMR (500 MHz, $CDCl_3$) δ 7.85 (d, J = 2.3 Hz, 2H), 7.63 (dd, J = 8.5, 5.5 Hz, 2H), 7.10 (t, J = 8.5 Hz, 2H), 3.98 – 3.93 (m, 2H), 3.92 – 3.87 (m, 2H), 2.96 (t, J = 7.4 Hz, 2H), 1.74 (h, J = 7.4 Hz, 2H), 1.02 (t, J = 7.4 Hz, 3H). ^{13}C NMR (125 MHz, $CDCl_3$) δ 173.82, 165.88, 164.09 (d, $J_{c\text{-f}}$ =250.02 Hz), 151.89, 144.42, 130.98, 130.50, 117.52, 116.04 (d, $J_{c\text{-f}}$ =21.75 Hz), 39.05, 38.74, 38.01, 17.75, 13.75. HRMS (ESI) *m/z* 327.1105 $[M+Na]^+$ (calcd for 327.1115, $C_{16}H_{17}FN_2NaO_3$).

(*E*)-1-(3-chloropropanoyl)-3-(3-(4-fluorophenyl) acryloyl) imidazolidin-2-one (***6i***)

Yield 26%, yellow powder. m.p. 190-192 °C. ^{1}H NMR (500 MHz, $CDCl_3$) δ 7.90 (d, J = 15.6 Hz, 1H), 7.83 (d, J = 15.6 Hz, 1H), 7.66 (dd, J = 8.7, 5.4 Hz, 2H), 7.15 (t, J = 8.7 Hz, 2H), 4.82 (s, 2H), 4.10 - 4.04 (m, 2H), 4.03 - 3.97 (m, 2H). ^{13}C NMR (125 MHz, $CDCl_3$) δ 166.70, 165.56, 164.24 (d, $J_{c\text{-f}}$ =250.75 Hz), 151.71, 145.21, 130.78, 130.53, 117.00, 116.15 (d, $J_{c\text{-f}}$ =21.88 Hz), 43.92, 39.55, 38.99. HRMS (ESI) *m/z* 333.0402 $[M+Na]^+$ (calcd for 333.0413, $C_{14}H_{12}ClFN_2NaO_3$).

(*E*)-1-(3-(4-fluorophenyl) acryloyl)-3-(thiophene-2-carbonyl) imidazolidin-2-one (***6j***)

Journal Pre-proof

Journal Pre-proof

Yield 36%, white powder. m.p. 145-147 °C. ^{1}H NMR (500 MHz, $CDCl_3$) δ 7.91 (dd, J = 3.9, 1.1 Hz, 1H), 7.83 (s, 1H), 7.83 (s, 1H), 7.68 (dd, J = 5.0, 1.1 Hz, 1H), 7.59 (dd, J = 8.7, 5.4 Hz, 2H), 7.15 (dd, J = 5.0, 3.9 Hz, 1H), 7.06 (t, J = 8.6 Hz, 2H), 4.04 (d, J = 1.4 Hz, 4H). ^{13}C NMR (125 MHz, $CDCl_3$) δ 165.85, 164.26 (d, $J_{c\text{-f}}$ =250.50 Hz), 162.82, 151.62, 144.68, 135.70, 134.83, 133.50, 130.91, 130.52, 127.36, 117.49, 116.02 (d, $J_{c\text{-f}}$ =250.50 Hz), 40.65, 39.48. HRMS (ESI) *m/z* 345.0695 $[M+H]^+$ (calcd for 345.0704 , $C_{17}H_{13}FN_2O_3S$).

(*E*)-1-benzoyl-3-(3-(4-fluorophenyl) acryloyl) imidazolidin-2-one (***6k***)

Yield 34%, white powder. m.p. 210-212 °C. ^{1}H NMR (500 MHz, $CDCl_3$) δ 7.82 (d, J = 15.7 Hz, 1H), 7.71 (d, J = 15.7 Hz, 1H), 7.67 (d, J = 7.5 Hz, 2H), 7.60 - 7.52 (m, 3H), 7.47 (t, J = 7.7 Hz, 2H), 7.03 (t, J = 8.6 Hz, 2H), 4.06 (s, 4H). ^{13}C NMR (125 MHz, $CDCl_3$) δ 170.29, 165.83, 164.09 (d, $J_{c\text{-f}}$ =250.50 Hz), 151.56, 144.74, 133.72, 132.24, 130.62, 130.55, 128.84, 127.98, 117.42, 115.95 (d, $J_{c\text{-f}}$ =21.75 Hz), 40.10, 39.44. HRMS (ESI) *m/z* 339.1125 $[M+H]^+$ (calcd for 339.1139, $C_{19}H_{15}FN_2O_3$).

(*E*)-4-(3-(3-(4-fluorophenyl) acryloyl)-2-oxoimidazolidine-1-carbonyl) benzonitrile (***6l***)

Yield 35%, white powder. m.p. 248-250 °C. ^{1}H NMR (500 MHz, $CDCl_3$) δ 7.83 (d, J = 15.7 Hz, 1H), 7.76 (d, J = 8.3 Hz, 2H), 7.71 (d, J = 8.2 Hz, 2H), 7.64 (d, J = 15.7 Hz, 1H), 7.54 (dd, J = 8.6, 5.4 Hz, 2H), 7.05 (t, J = 8.6 Hz, 2H), 4.07 (q, J = 2.3 Hz, 4H). ^{13}C NMR (125 MHz, $CDCl_3$) δ 168.55, 165.60, 164.20 (d, $J_{c\text{-f}}$ =250.75 Hz), 151.34, 145.27, 137.89, 131.77, 130.67, 130.57, 129.11, 117.99, 116.93, 116.06 (d, J

Journal Pre-proof

$_{c\text{-f}}$ =21.88 Hz), 115.38, 39.78, 39.44. HRMS (ESI) *m/z* 386.0905 $[M+Na]^+$ (calcd for 386.0911, $C_{20}H1_4FN_3NaO_3$).

N-ethyl-3-(3-(4-fluorophenyl)propanoyl)-N-methyl-2-oxoimidazolidine-1-carboxamide (***6m***)

Yield 30%, white powder. m.p. 156-158 °C. ^{1}H NMR (600 MHz, $CDCl_3$) δ 7.21 (dd, *J* = 8.3, 5.5 Hz, 2H), 6.97 (t, *J* = 8.7 Hz, 2H), 3.87 (t, *J* = 7.8 Hz, 2H), 3.78 (d, *J* = 8.1 Hz, 2H), 3.44 (d, *J* = 7.1 Hz, 2H), 3.23 (t, *J* = 7.6 Hz, 2H), 3.00 (s, 3H), 2.97 (t, *J* = 7.6 Hz, 2H), 1.22 (d, *J* = 7.2 Hz, 3H). ^{13}C NMR (125 MHz, $CDCl_3$) δ 172.62, 161.43 (d, $J_{c\text{-f}}$ =242.38 Hz), 153.71, 152.19, 136.39, 129.92, 115.13 (d, $J_{c\text{-f}}$ =21.00 Hz), 41.69, 40.62, 39.72, 37.49, 29.62, 27.15, 12.31. HRMS (ESI) *m/z* 344.1383 $[M+Na]^+$ (calcd for 344.1381, $C_{16}H_{20}FN_3O_3$).

5. Author Information

* Correspondence Author

*Xiao-BingWang. Tel/ Fax: +86-25-8327-1402. E-mail address: xbwang@cpu.edu.cn

* Ling-Yi Kong. Tel/ Fax: +86-25-8327-1405. E-mail address: cpu_lykong@126.com

6. Acknowledgments

This work was supported by the National Natural Science Foundation of China (81573313), the "Double First-Class" University Project (CPU2018GF03), Jiangsu Province ‘333’ Project (Wang, X.B.), the Qinglan Project of Jiangsu Province of China (Wang, X. B.), the Six Talent Peaks Project of Jiangsu Province (SWYY-107), and the Innovative Research Team in University (IRT_15R63).

References

Journal Pre-proof

[1] F. Luo, A.F. Sandhu, W. Rungratanawanich, G.E. Williams, M. Akbar, S. Zhou, B.J. Song, X. Wang, Melatonin and Autophagy in Aging-Related Neurodegenerative Diseases, *Int J Mol Sci*, 21 (2020).

[2] B. Uttara, A. V. Singh, P. Zamboni, R.T. Mahajan, Oxidative stress and neurodegenerative diseases: a review of upstream and downstream antioxidant therapeutic options. *Curr. Neuropharmacol.* 7 (2009), 65−74.

[3] J. Emerit, M. Edeas, F. Bricaire, Neurodegenerative diseases and oxidative stress, *Biomedicine & Pharmacotherapy*, 58 (2004) 39-46.

[4] X. Gu, J. Chen, Y. Zhang, M. Guan, X. Li, Q. Zhou, Q. Song, J. Qiu, Synthesis and assessment ofphenylacrylamide derivatives as potential anti-oxidant and anti-inflammatory agents, *Eur J Med Chem*, 180 (2019) 62-71.

[5] L. Wang, X. Cai, M. Shi, L. Xue, S. Kuang, R. Xu, W. Qi, Y. Li, X. Ma, R. Zhang, F. Hong, H. Ye, L. Chen, Identification and optimization of piperine analogues as neuroprotective agents for the treatment of Parkinson's disease via the activation of Nrf2/keap1 pathway, *Eur J Med Chem*, 199 (2020) 112385.

[6] D.A. Johnson, J.A. Johnson, Nrf2—a therapeutic target for the treatment of neurodegenerative diseases, *Free Radic Biol Med*, 88 (2015) 253-267.

[7] L. Pruccoli, F. Morroni, G. Sita, P. Hrelia, A. Tarozzi, Esculetin as a Bifunctional Antioxidant Prevents and Counteracts the Oxidative Stress and Neuronal Death Induced by Amyloid Protein in SH-SY5Y Cells, *Antioxidants (Basel)*, 9 (2020).

[8] T. Y. Kim, E. Leem, J. M. Lee, Control of Reactive Oxygen Species for the Prevention of Parkinson's Disease: The Possible Application of Flavonoids, *Antioxidants (Basel)*, 2020 9(7): 583.

[9] S.Y. Woo, J.H. Kim, M.K. Moon, S.H. Han, S.K. Yeon, J.W. Choi, B.K. Jang, H.J. Song, Y.G. Kang, J.W. Kim, J. Lee, D.J. Kim, O. Hwang, K.D. Park, Discovery of Vinyl Sulfones as a Novel Class of Neuroprotective Agents toward Parkinson's Disease Therapy, *J Med Chem*, 57 (2014) 1473-1487.

[10] S. Peng, B. Zhang, X. Meng, J. Yao, J. Fang, Synthesis of Piperlongumine Analogues and Discovery of Nuclear Factor Erythroid 2□Related Factor 2 (Nrf2) Activators as Potential Neuroprotective Agent, *J Med Chem*, 58 (2015) 5242-5255.

[11] M. Dodson, M.R. de la Vega, A.B. Cholanians, C.J. Schmidlin, E. Chapman, D.D. Zhang, Modulating NRF2 in Disease: Timing Is Everything, *Annu Rev Pharmacol Toxicol*, 59 (2019) 555-575.

[12] L. Fao, S.I. Mota, A.C. Rego, Shaping the Nrf2-ARE-related pathways in Alzheimer's and Parkinson's disease, *Ageing Res Rev*, 54 (2019) 100942.

[13] L. Subedi, J.H. Lee, S. Yumnam, E. Ji, S.Y. Kim, Anti-Inflammatory Effect of Sulforaphane on LPS-ActivatedMicroglia Potentially through JNK/AP-1/ NF-κB Inhibition and Nrf2/HO-1 Activation, *Cells*, 8 (2019).

Journal Pre-proof

Journal Pre-proof

[14] X. Gu, J. Chen, Y. Zhang, M. Guan, X. Li, Q. Zhou, Q. Song, J. Qiu, Synthesis and assessment ofphenylacrylamide derivatives as potential antioxidant and anti-inflammatory agents, *Eur J Med Chem*, 180 (2019) 62-71.

[15] J. Yan, Y. Pang, J. Zhuang, H. Lin, Q. Zhang, L. Han, P. Ke, J. Zhuang, X. Huang, Selenepezil, a selenium-containing compound, exerts neuroprotective effect via modulation of Keap1-Nrf2-ARE pathway and attenuates A#-induced cognitive impairment in vivo, *ACS Chem Neurosci*, 10 (2019) 2903-2914.

[16] S. Li, C. Takasu, H. Lau, L. Robles, K. Vo, T. Farzaneh, N.D. Vaziri, M.J. Stamos, H. Ichii, Dimethyl Fumarate Alleviates Dextran Sulfate Sodium-Induced Colitis, through the Activation of Nrf2-Mediated Antioxidant and Anti-inflammatory Pathways, *Antioxidants (Basel)*, 9 (2020).

[17] K.E. Carlstrom, P.K. Chinthakindi, B. Espinosa, F. Al Nimer, E.S.J. Arner, P.I. Arvidsson, F. Piehl, K. Johansson, Characterization of More Selective Central Nervous System Nrf2-Activating Novel Vinyl Sulfoximine Compounds Compared to Dimethyl Fumarate, *Neurotherapeutics*, (2020).

[18] J. Yao, B. Zhang, C. Ge, S. Peng, J. Fang, Xanthohumol, a polyphenol chalcone present in hops, activating Nrf2 enzymes to confer protection against oxidative damage in PC12 cells, *J Agric Food Chem*, 63 (2015) 1521-1531.

Journal Pre-proof

[19] F. Bai, B. Zhang, Y. Hou, J. Yao, Q. Xu, J. Xu, J. Fang, Xanthohumol Analogues as Potent Nrf2 Activators against Oxidative Stress Mediated Damages of PC12 Cells, *ACS Chem Neurosci*, 10 (2019) 2956-2966.

[20] Y. Zhuang, H. Wu, X. Wang, J. He, S. He, Y. Yin, Resveratrol Attenuates Oxidative Stress-Induced Intestinal Barrier Injury through PI3K/Akt-Mediated Nrf2 Signaling Pathway, *Oxid Med Cell Longev*, 2019 (2019) 7591840.

[21] D.S. Lee, G.S. Jeong, Butein provides neuroprotective and antineuroinflammatory effects through Nrf2/ARE-dependent haem oxygenase 1 expression by activating 3K/Akt pathway, *Br J Pharmacol*, 173 (2016) 2894-2909.

[22] C. Pang, Z. Zheng, L. Shi, Y. Sheng, H. Wei, Z. Wang, L. Ji, Caffeic acid prevents acetaminophen-induced liver injury by activating the Keap1-Nrf2 antioxidative defense system, *Free Radic Biol Med*, 91 (2016) 236-246.

[23] S. Chen, S. Yang, M. Wang, J. Chen, S. Huang, Z. Wei, Z. Cheng, H. Wang, M. Long, P. Li, Curcumin inhibits zearalenone-induced apoptosis and oxidative stress in Leydig cells via modulation of the PTEN/Nrf2/Bip signaling pathway, *Food Chem Toxicol*, 141 (2020) 111385.

[24] A.J. Wilson, J.K. Kerns, J.F. Callahan, C.J. Moody, Keap calm, and carry on covalently, *J Med Chem*, 56 (2013) 7463-7476.

Journal Pre-proof

Journal Pre-proof

[25] J. Go, T.-K.-Q. Ha, J.Y. Seo, T.-S. Park, Y.-K. Ryu, H.-Y. Park, J.-R. Noh, Y.-H. Kim, J.H. Hwang, D.-H. Choi, D.Y. Hwang, S. Kim, C.-H. Lee, W.K. Oh, K.-S. Kim, Piperlongumine activates Sirtuin1 and improves cognitive function in a murine model of Alzheimer's disease, *Journal of Functional Foods*, 43 (2018) 103-111.

[26] K. Piska, A. Gunia-Krzyzak, P. Koczurkiewicz, K. Wojcik-Pszczola, E. Pekala, Piperlongumine (piplartine) as a lead compound for anticancer agents e Synthesis and properties of analogues: A mini-review, *Eur J Med Chem*, 156 (2018) 13-20.

[27] J. Wiemann, J. Karasch, A. Loesche, L. Heller, W. Brandt, R. Csuk, Piperlongumine B and analogs are promising and selective inhibitors for acetylcholinesterase, *Eur J Med Chem*, 139 (2017) 222-231.

[28] J. Go, T.-K.-Q. Ha, J.Y. Seo, T.-S. Park, Y.-K. Ryu, H.-Y. Park, J.-R. Noh, Y.-H. Kim, J.H. Hwang, D.-H. Choi, D.Y. Hwang, S. Kim, C.-H. Lee, W.K. Oh, K.-S. Kim, Piperlongumine activates Sirtuin1 and improves cognitive function in a murine model of Alzheimer's disease, *Journal of Functional Foods*, 43 (2018) 103-111.

[29] X. Liu, Y. Wang, X. Zhang, Z. Gao, S. Zhang, P. Shi, X. Zhang, L. Song, H. Hendrickson, D. Zhou, G. Zheng, Senolytic activity of piperlongumine analogues: Synthesis and biological evaluation, *Bioorg Med Chem*, 26 (2018) 3925-3938.

Journal Pre-proof

[30] G. Li, Y. Zheng, J. Yao, L. Hu, Q. Liu, F. Ke, W. Feng, Y. Zhao, P. Yan, W. He, H. Deng, P. Qiu, W. Li, J. Wu, Design and Green Synthesis of Piperlongumine Analogs and Their Antioxidant Activity against Cerebral Ischemia-Reperfusion Injury, *ACS Chem Neurosci*, 10 (2019) 4545-4557.

[31] Y. Hou, S. Peng, X. Li, J. Yao, J. Xu, J. Fang, Honokiol Alleviates Oxidative Stress-Induced Neurotoxicity via Activation of Nrf2, *ACS Chem Neurosci*, 9 (2018) 3108-3116.

[32] J.H. Woo, J.H. Lee, H. Kim, S.J. Park, E. Joe, I. Jou, Control of Inflammatory Responses: a New Paradigm for the Treatment of Chronic Neuronal Diseases, *Exp Neurobiol*, 24 (2015) 95-102.

[33] D. J. Bonda, X. L.Wang, G. Perry, A. Nunomura, M. Tabaton. Oxidative stress in Alzheimer disease: a possibility for prevention. *Neuropharma*. 2010, 59, 290−294.

[34] J. Yan, Y. Pang, J. Zhuang, H. Lin, Q. Zhang, L. Han, P. Ke, J. Zhuang, X. Huang, Selenepezil, a selenium-containing compound, exerts neuroprotective effect via modulation of Keap1-Nrf2-ARE pathway and attenuates A#-induced cognitive impairment in vivo, *ACS Chem Neurosci*, 10 (2019) 2903-2914.

[35] J.H. Woo, J.H. Lee, H. Kim, S.J. Park, E. Joe, I. Jou, Control of Inflammatory Responses: a New Paradigm for the Treatment of Chronic Neuronal Diseases, *Exp Neurobiol*, 24 (2015) 95-102.

Journal Pre-proof

[36] B. Kadenbach, S. Arnold, I. Lee, M. Hüttemann, The possible role of cytochrome c oxidase in stress-induced apoptosis and degenerative diseases, Biochimica et biophysica acta. *Bioenergetics*, 1655 (2004) 400-408.

[37] T. Wyss-Coray, Inflammation in Alzheimer disease: driving force, bystander or beneficial response?, *Nature Medicine*, 12 (2006) 1005-1015.

[38] H.J. Kim, B.K. Jang, J.H. Park, J.W. Choi, S.J. Park, S.R. Byeon, A.N. Pae, Y.S. Lee, E. Cheong, K.D. Park, A novel chalcone derivative as Nrf2 activator attenuates learning and memory impairment in a scopolamine-induced mouse model, Eur J Med Chem, 185 (2020) 111777.

[39] R. Scherer, H. T. Godoy. Antioxidant activity index (AAI) by the 2,2-diphenyl-1-picrylhydrazyl method. *Food Chem*. 2009, 112, 654-658.

[40] N. J. Mille, C. A. Riceevans. Factors influencing the antioxidant activity determined by the ABTS•+ radical cation assay, *Free Radical Res*. 1997, 26 195−199.

[41] C. Zhuang, S. Narayanapillai, W. Zhang, Y.Y. Sham, C. Xing, Rapid identification of Keap1-Nrf2 small-molecule inhibitors through structure-based virtual screening and hit-based substructure search, *J Med Chem*, 57 (2014) 1121-1126.

Journal Pre-proof

Journal Pre-proof

[42] C.J. Shi, W. Peng, J.H. Zhao, H.L. Yang, L.L. Qu, C. Wang, L.Y. Kong, X.B. Wang, Usnic acid derivatives as tau-aggregation and neuroinflammation inhibitors, *Eur J Med Chem*, 187 (2020) 111961.

[43] J.Egeaa, I. Buendiaa, E.Paradaa, E.Navarroa, R.Leóna, M.G. Lopez. Anti-inflammatory role of microglial alpha7 nAChRs and its role in neuroprotection. *Biochem. Pharmacol*. 2015, 97, 463−472.

[44] S.M. Ahmed, L. Luo, A. Namani, X.J. Wang, X. Tang, Nrf2 signaling pathway: pivotal roles in inflflammation, Biochim. Biophys. *Acta (BBA) - Mol. Basis Dis*. 1863 (2017) 585-597.

[45] T.W. Lee, E. Bae, J.H. Kim, H.N. Jang, H.S. Cho, S.H. Chang, D.J. Park, The aqueous extract of aged black garlic ameliorates colistin-induced acute kidney injury in rats, *Ren. Fai*l. 41 (2019) 24-33.

[46] N.H. Dang, Y.Y. Choo, N.T. Dat, N.H. Nam, V.M. Chau, J.H. Lee, 7-Methoxy-(9H-beta-Carbolin-1-il)-(E)-1-Propenoic acid, a beta-carboline alkaloid from eurycoma longifolia, exhibits anti-inflflammatory effects by activating the Nrf2/ heme oxygenase-1 pathway, *J. Cell. Biochem*. 117 (2016) 659-670.

[47] M.C. Lu, X. Zhang, F. Wu, S.J. Tan, J. Zhao, Q.D. You, Z.Y. Jiang, Discovery of a Potent Kelch-Like ECH-Associated Protein 1-Nuclear Factor Erythroid 2-Related Factor 2 (Keap1-Nrf2) Protein-Protein Interaction Inhibitor with

Journal Pre-proof

Natural Proline Structure as a Cytoprotective Agent against Acetaminophen-Induced Hepatotoxicity, *J Med Chem*, 62 (2019) 6796-6813

[48] Z.Y. Jiang, L.L. Xu, M.C. Lu, Z.Y. Chen, Z.W. Yuan, X.L. Xu, X.K. Guo, X.J. Zhang, H.P. Sun, Q.D. You, Structure-Activity and Structure-Property Relationship and Exploratory in Vivo Evaluation of the Nanomolar Keap1-Nrf2 Protein-Protein Interaction Inhibitor, *J Med Chem*, 58 (2015) 6410-6421.

[49] Y. Li, O. Lv, F. Zhou, Q. Li, Z. Wu, Y. Zheng, Linalool Inhibits LPS-Induced Inflammation in BV2 Microglia Cells by Activating Nrf2, *Neurochem Res*, 40 (2015) 1520-1525.

[50] S. Peng, Y. Hou, J. Yao, J. Fang, Activation of Nrf2 by costunolide provides neuroprotective effect in PC12 cells, *Food Funct*, 10 (2019) 4143-4152.

[51] J.W. Choi, S. Kim, J.H. Park, H.J. Kim, S.J. Shin, J.W. Kim, S.Y. Woo, C. Lee, S.M. Han, J. Lee, A.N. Pae, G. Han, K.D. Park, Optimization of Vinyl Sulfone Derivatives as Potent Nuclear Factor Erythroid 2□Related Factor 2 (Nrf2) Activators for Parkinson's Disease Therapy, *J Med Chem*, 62 (2019) 811-830.

[52] Z.Y. Jiang, M.C. Lu, L.L. Xu, T.T. Yang, M.Y. Xi, X.L. Xu, X.K. Guo, X.J. Zhang, Q.D. You, H.P. Sun, Discovery of potent Keap1-Nrf2 protein-protein interaction inhibitor based on molecular binding determinants analysis, *J Med Chem*, 57 (2014) 2736-2745.

Journal Pre-proof

[53] L. Di, E.H. Kerns, K. Fan, O.J. McConnell, G.T. Carter, High throughput artificial membrane permeability assay for blood-brain barrier, *Eur J Med Chem*, 38 (2003) 223-232.

Journal Pre-proof

Table 1 The neuroprotection of PL analogues substituted with different aryl group

Compd.	Structure	Cell viability (%)	
		H_2O_2	6-OHDA
Model		46.00 ± 4.12	45.23 ± 4.37
1	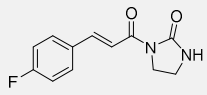	68.57 ± 2.88	69.13 ± 3.4
2	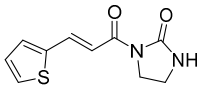	65.15 ± 3.86	64.2 ± 1.74
3	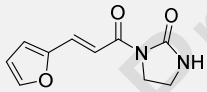	64.08 ± 3.55	60.00 ± 2.72
4	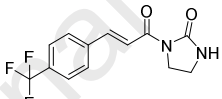	67.66 ± 4.15	65.32 ± 4.72
5	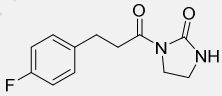	53.56 ± 1.29	56.32 ± 2

[a] Cell viability (%) of PC12 cells were detected by the MTT assay after 24 h of incubation with compounds at the concentration of 20 μM with H_2O_2 (200 μM) or 6-OHDA (150 μM). Data are the mean ± SD of three independent experiments.

Journal Pre-proof

Table 2 The neuroprotection of PL analogues substituted with different aryl group

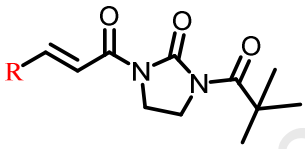

Compd.	R	Cell viability (%)[a]		Compd.	R	Cell viability (%)	
		H_2O_2	6-OHDA			H_2O_2	6-OHDA
Model		46.00 ± 4.12	45.23 ± 4.37	**17**		70.01 ± 4.55	69.01 ± 2.39
6		73.58 ± 3.55	72.23 ± 2.72	**18**		69.21 ± 1.87	68.32 ± 4.06
7	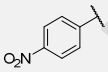	70.15 ± 3.86	69.21 ± 0.74	**19**		60.36 ± 2.42	56.73 ± 1.30
8	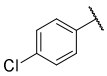	72.05 ± 2.15	71.12 ± 3.23	**20**		69.66 ± 4.15	68.31 ± 4.72
9	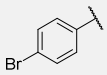	72.22 ± 2.11	70.79 ± 2.82	**21**		69.23 ± 3.86	68.21 ± 4.55
10	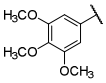	72.1 8 ± 0.76	72.32 ± 2.25	**22**		70.91 ± 5.32	69.58 ± 2.51
11	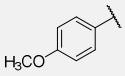	71.14 ± 1.81	70.32 ± 3.09	**23**		71.41 ± 4.5	71.12 ± 4.02

Journal Pre-proof

12	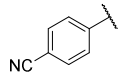	61.52 ± 3.22	60.08 ± 5.27	**24**		72.33 ± 3.54	71.79 ± 5.49
13		70.97 ± 2.54	69.32 ± 4.19	**25**	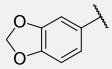	63.33 ± 1.05	62.31 ± 2.94
14		72.43 ± 2.54	72.33 ± 1.20	**26**		59.15 ± 4.34	56.38 ± 5.36
15	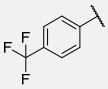	72.5 ± 2.88	71.12 ± 3.40	**27**	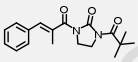	73.22 ± 2.73	72.13 ± 6.40
16	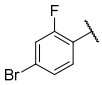	63.55 ± 1.64	61.77 ± 2.54	**28**	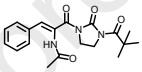	72.65 ± 4.48	71.21 ± 2.62

[a] Cell viability (%) of PC12 cells were detected by the MTT assay after 24 h of incubation with compounds at the concentration of 20 μM with H_2O_2 (200 μM) or 6-OHDA (150 μM). Data are the mean ± SD of three independent experiments.

Table 3 The neuroprotection of **PL** analogues substituted with different groups

Compd.	**Structure**	**Cell viability (%)[a]**	
		(H_2O_2-induced)	**(6-OHDA-induced)**
Model		46.96 ± 4.12	45.65 ± 4.37
6a	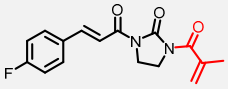	38.05 ± 3.20	30.23 ± 4.35
6b	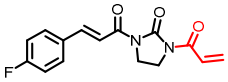	43.96 ± 5.43	43.76 ± 5.01

Journal Pre-proof

6c	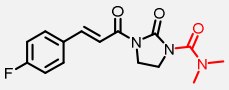	73.82 ± 1.39	71.32 ± 2.87
6d	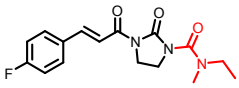	75.01 ± 2.02	75.44 ± 2.29
6e	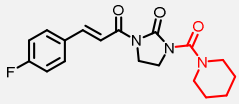	72.8 ± 1.19	72.14 ± 2.60
6f	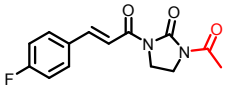	70.42 ± 4.51	72.27 ± 2.21
6g	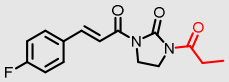	71.58 ± 4.55	70.23 ± 3.72
6h	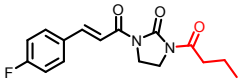	70.15 ± 3.86	69.26 ± 1.74
6i	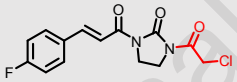	43.25 ± 4.15	37.12 ± 3.23
6j	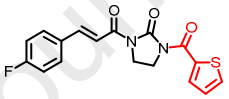	62.25 ± 2.11	60.79 ± 2.82
6k	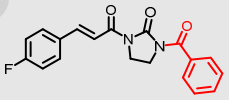	63.28 ± 0.76	60.32 ± 5.25
6l	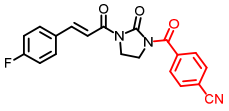	55.14 ± 4.81	52.32 ± 2.09
6m	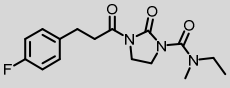	59.5 ± 4.20	62.45± 1.20

[a] Cell viability (%) of PC12 cells were detected by the MTT assay after 24 h of incubation with compounds at the concentration of 20 μM with H_2O_2 (200 μM) or

Journal Pre-proof

6-OHDA (150 μM). Data are the mean ± SD of three independent experiments.

Journal Pre-proof

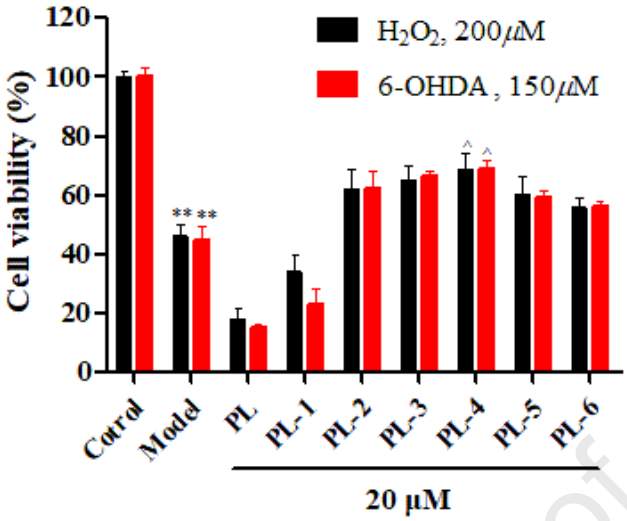

Figure 1 Initial screening of PL analogues against 6-OHDA- or H_2O_2-induced PC12 cell damage. Data are the mean ± SD of three independent experiments. (**p) ≤ 0.01 compared with the control group; ($^{\wedge}$p) ≤ 0.05 compared with H_2O_2-treated or 6-OHDA-treated group.

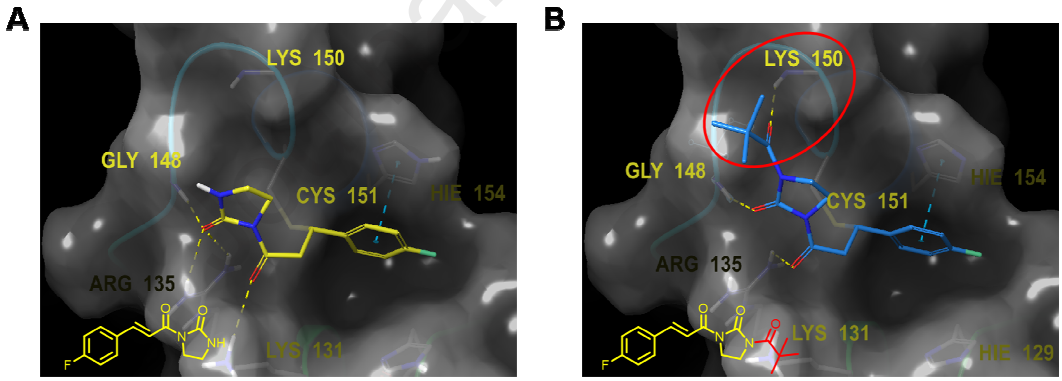

Figure 2. The docking models of icompond **1** (A) and **6** (B) with the BTB domain of Keap1 (PDB: 4CXT).

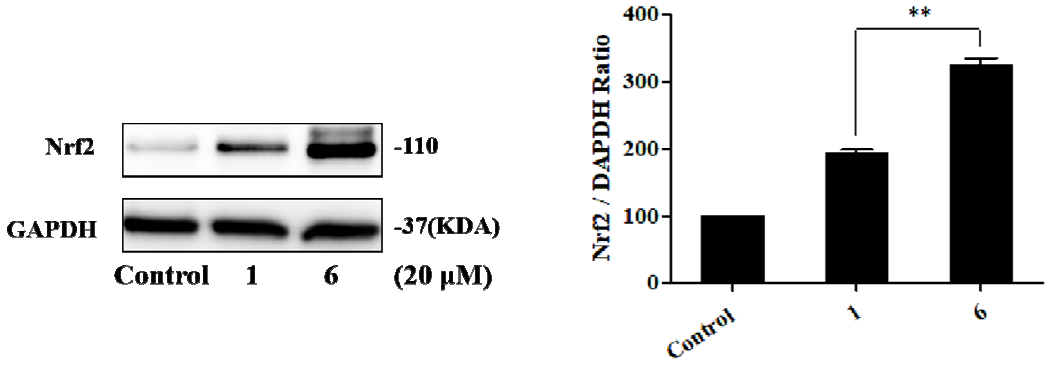

Figure 3 The expression of Nrf2 in PC12 cells after treatment with compounds **1** and **6.** (**p) ≤ 0.05, Data are presented by mean ± SD (n = 3).

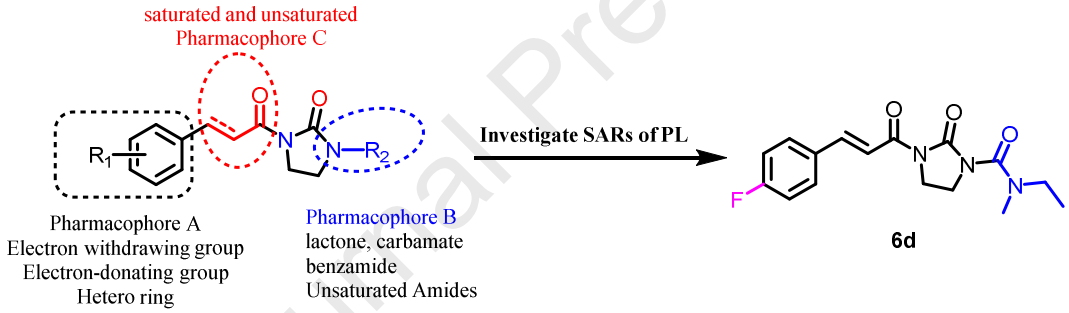

Figure 4 The design of the modifications of **PL**

Journal Pre-proof

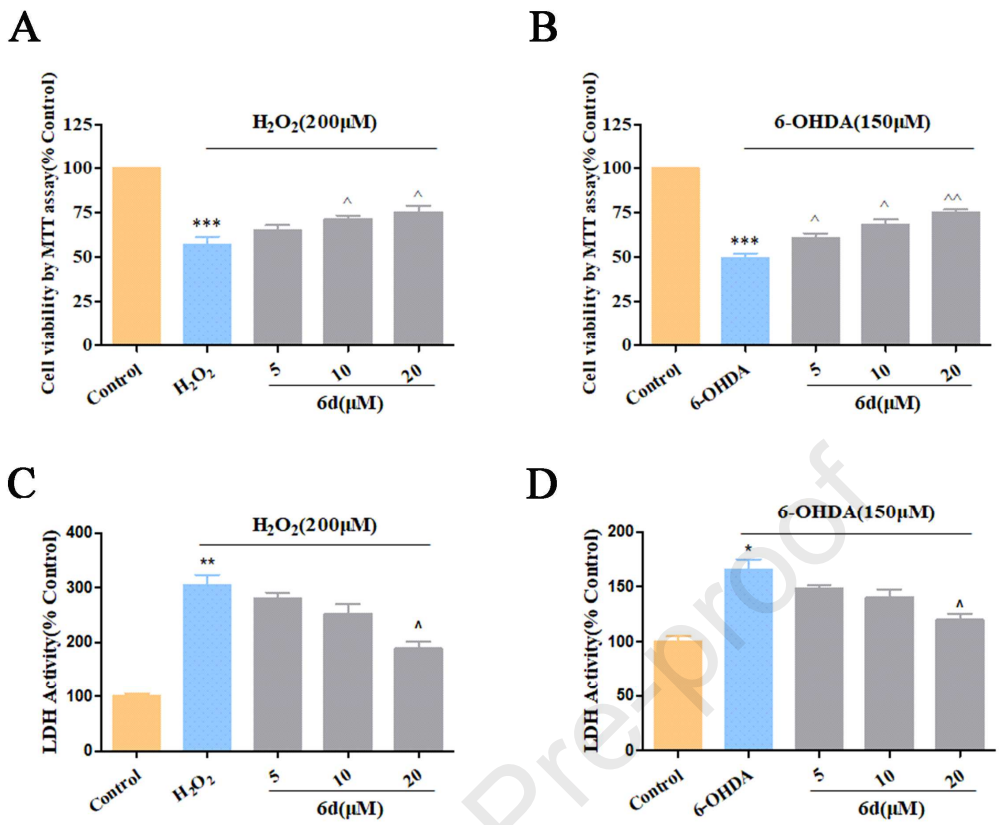

Figure 5. Protection of **6d** against H_2O_2- (A) and 6-OHDA-induced (B) PC12 cell damage, determined by MTT assay. Protection of **6d** against H_2O_2-induced (C) and 6-OHDA-induced (D) PC12 cell damage was measured by the LDH release assay. Data are the mean ± SD of three independent experiments. (**p) ≤ 0.01 and (***p) ≤ 0.001 compared with the control group; (^p) ≤ 0.05, (^^p) ≤ 0.01 and (^^^p) ≤ 0.001 compared with H_2O_2-treated or 6-OHDA-treated group.

Journal Pre-proof

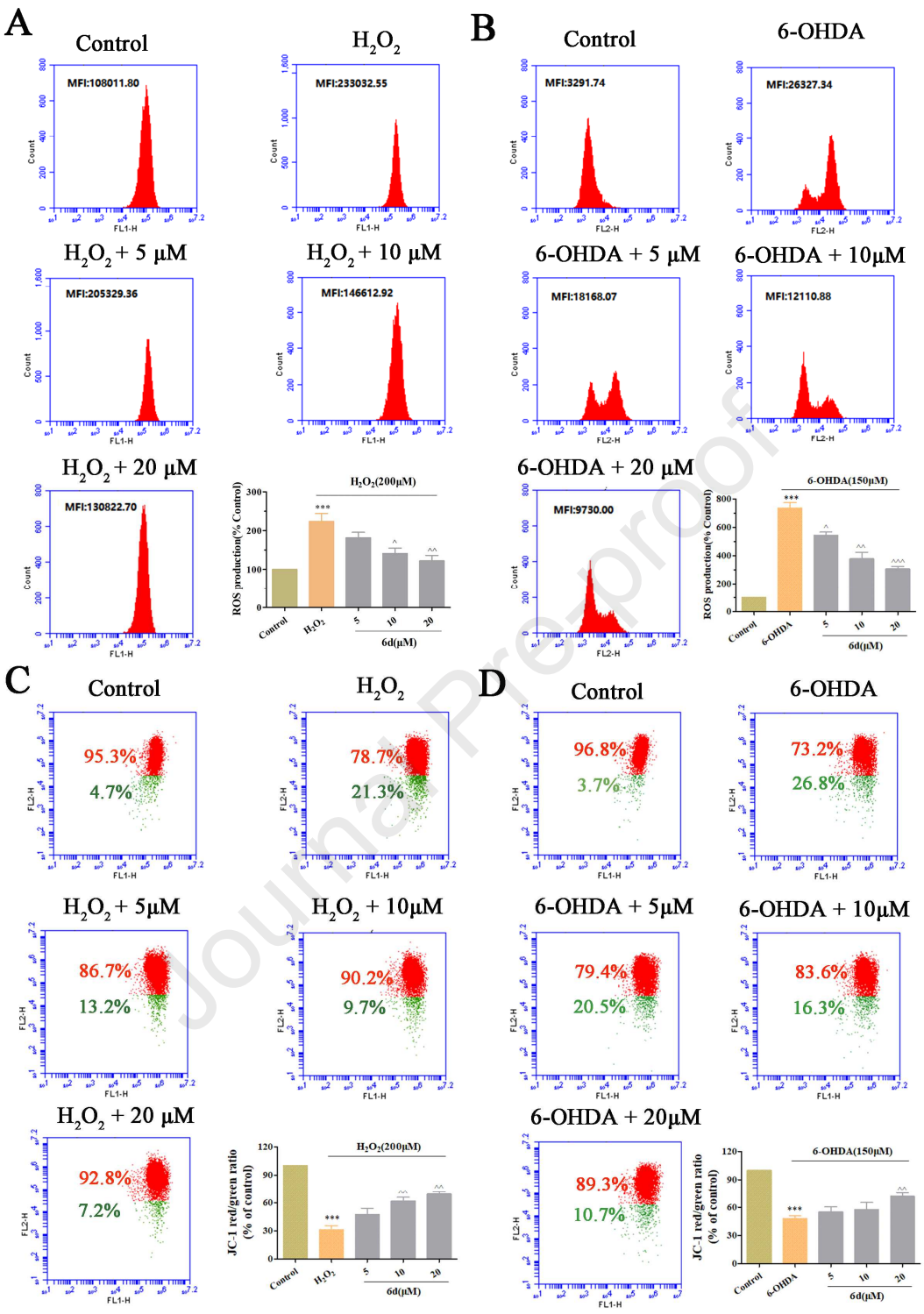

Figure 6. The effects of **6d** on H_2O_2-induced (A) and 6-OHDA-induced (B) intracellular ROS production in PC12 cells. The cells were stained with DCFH-DA and immediately determined by flow cytometry. The effects of **6d** on

H_2O_2-induced (C) and 6-OHDA-induced (D) MMP reduction in PC12 cells. MMP were detected by flow cytometry after JC-1 staining. Data are presented by mean ± SD (n = 3). (***p) ≤ 0.001 compared with the control group; (^p) ≤ 0.05, (^^p) ≤ 0.01 and (^^^p) ≤ 0.001 compared with H_2O_2-treated or 6-OHDA-treated group.

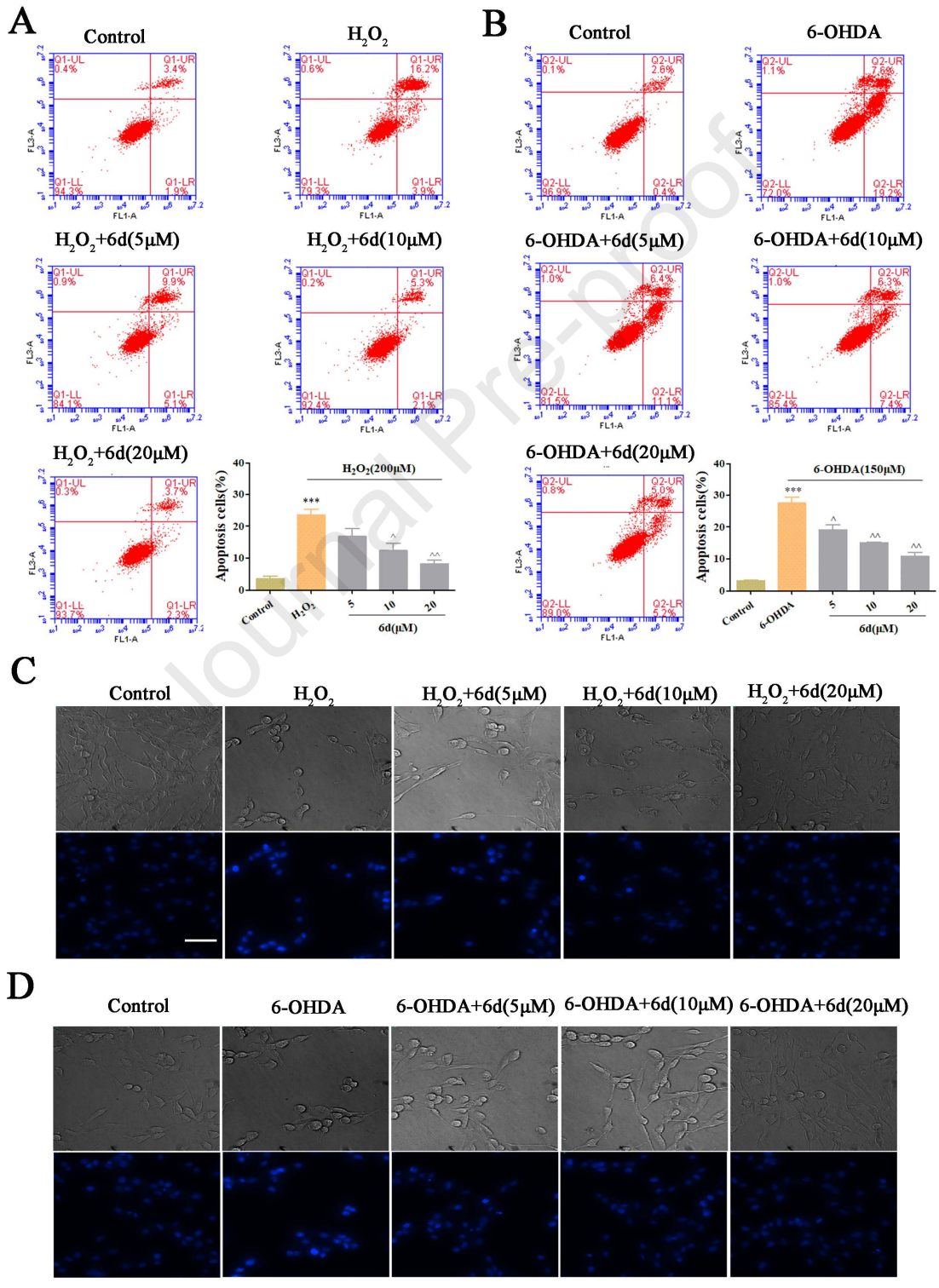

Figure 7. Prevention of PC12 cells from H_2O_2-induced (A) and 6-OHDA-induced (B) apoptosis by **6d**. Apoptotic cells were detected by flow cytometry after AnnexinV and PI double staining. (C, D) Images showed the apoptotic nuclei by Hoechst 33342 staining. The top panel is phase contrast pictures, and the bottom panel is fluorescent pictures. Scale bars: 100 μm. Data are presented by mean ± SD (n = 3). (***p) ≤ 0.001 compared with the control group; (^p) ≤ 0.05 and (^^p) ≤ 0.01 compared with H_2O_2- or 6-OHDA-treated group.

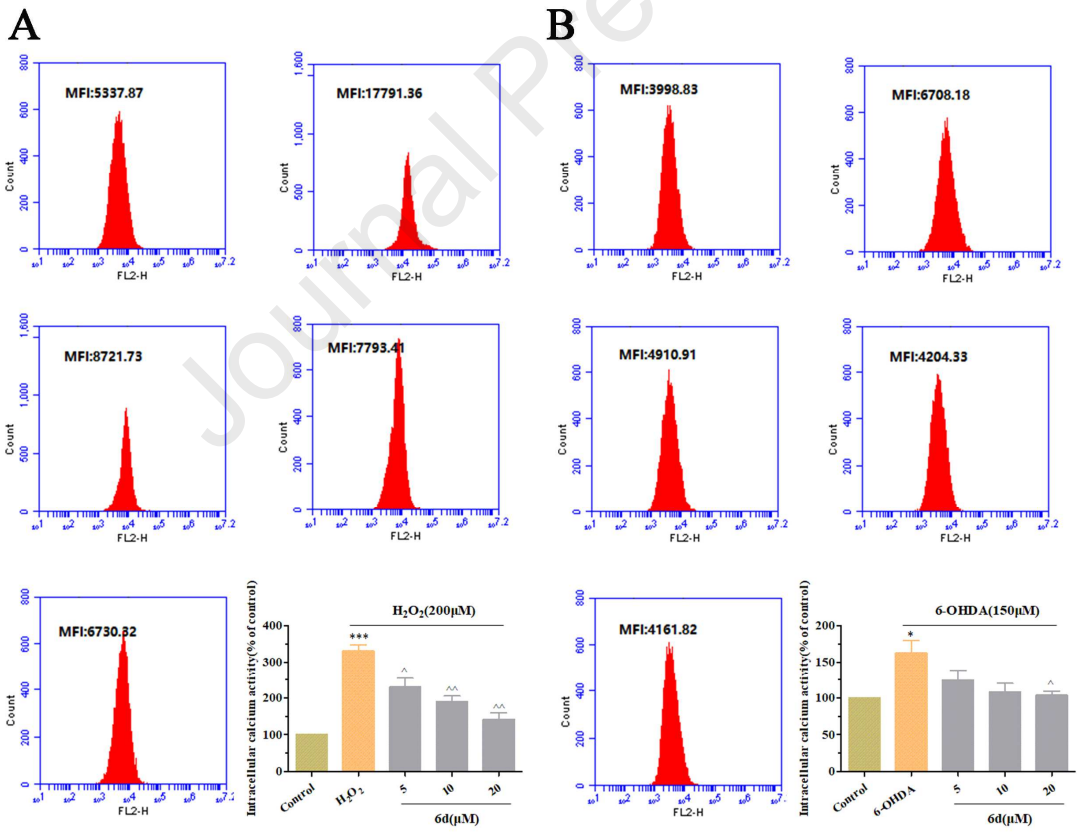

Figure 8. Effects of **6d** on H_2O_2-induced (A) and 6-OHDA-induced (B) Ca^{2+} overload in PC12 cells. Data are presented by mean ± SD (n = 3). (*p) ≤ 0.05 and (***p) ≤ 0.001 compared with the control group; (^p) ≤ 0.05 and (^^p) ≤ 0.01

compared with H_2O_2-treated or 6-OHDA-treated group.

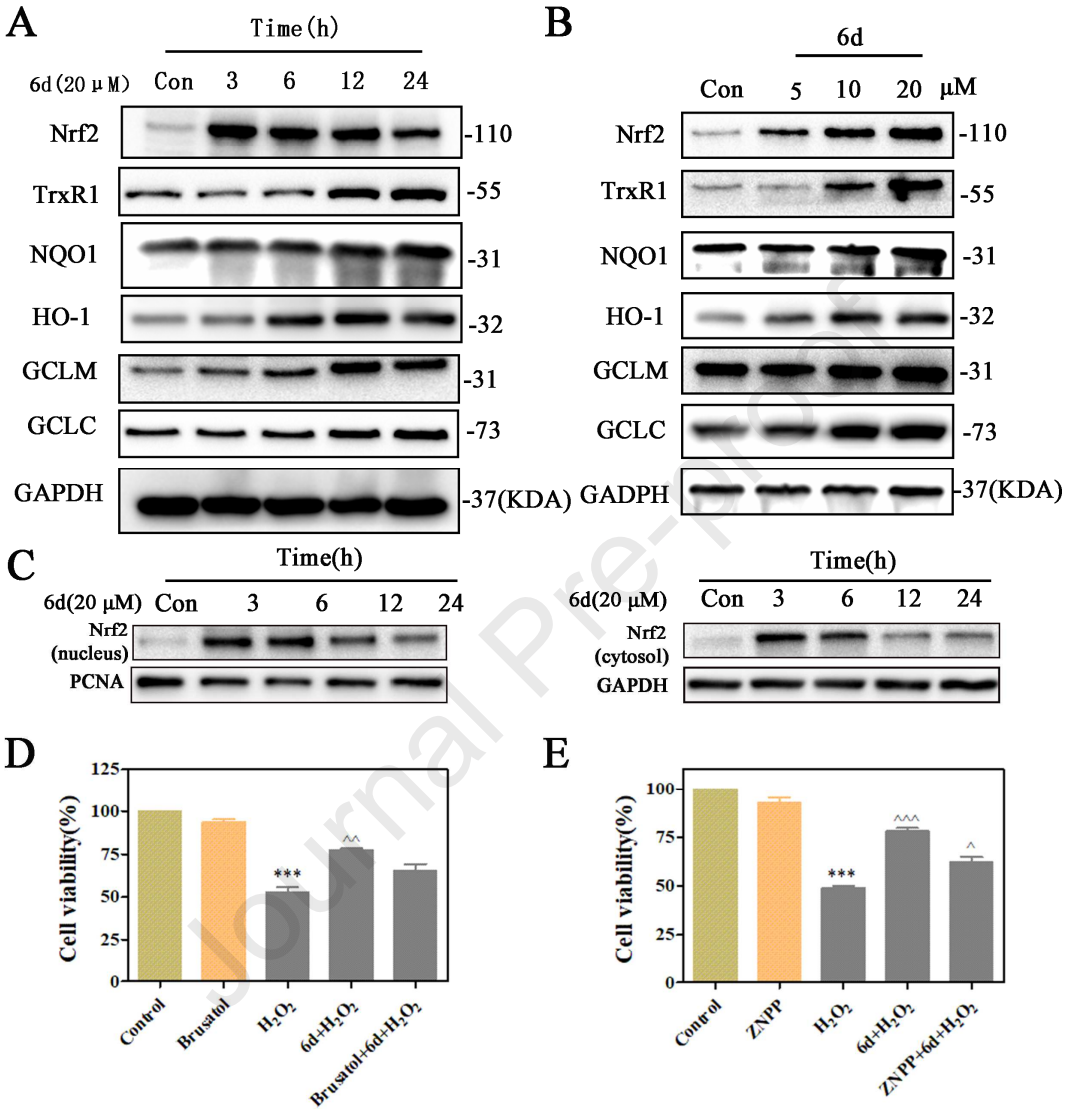

Figure 9. 6d could increase the expression of nuclear and cytosolic Nrf2, TrxR1, NQO-1, HO-1, GCLM and GCLC in a time (A) and dose (B) dependent manner. Promotion of Nrf2 nuclear accumulation by **6d** (C). Brusatol (D), ZnPP (E) affected the protection of **6d**. PC12 cells were incubated for 30 min in the presence of **6d** (20 μM) together with brusatol (10 nM) or ZNPP (10 nM) prior to stimulation with H_2O_2 (150 μM) for 24 h, determined by MTT assay. Data are

presented by mean ± SD (n = 3).

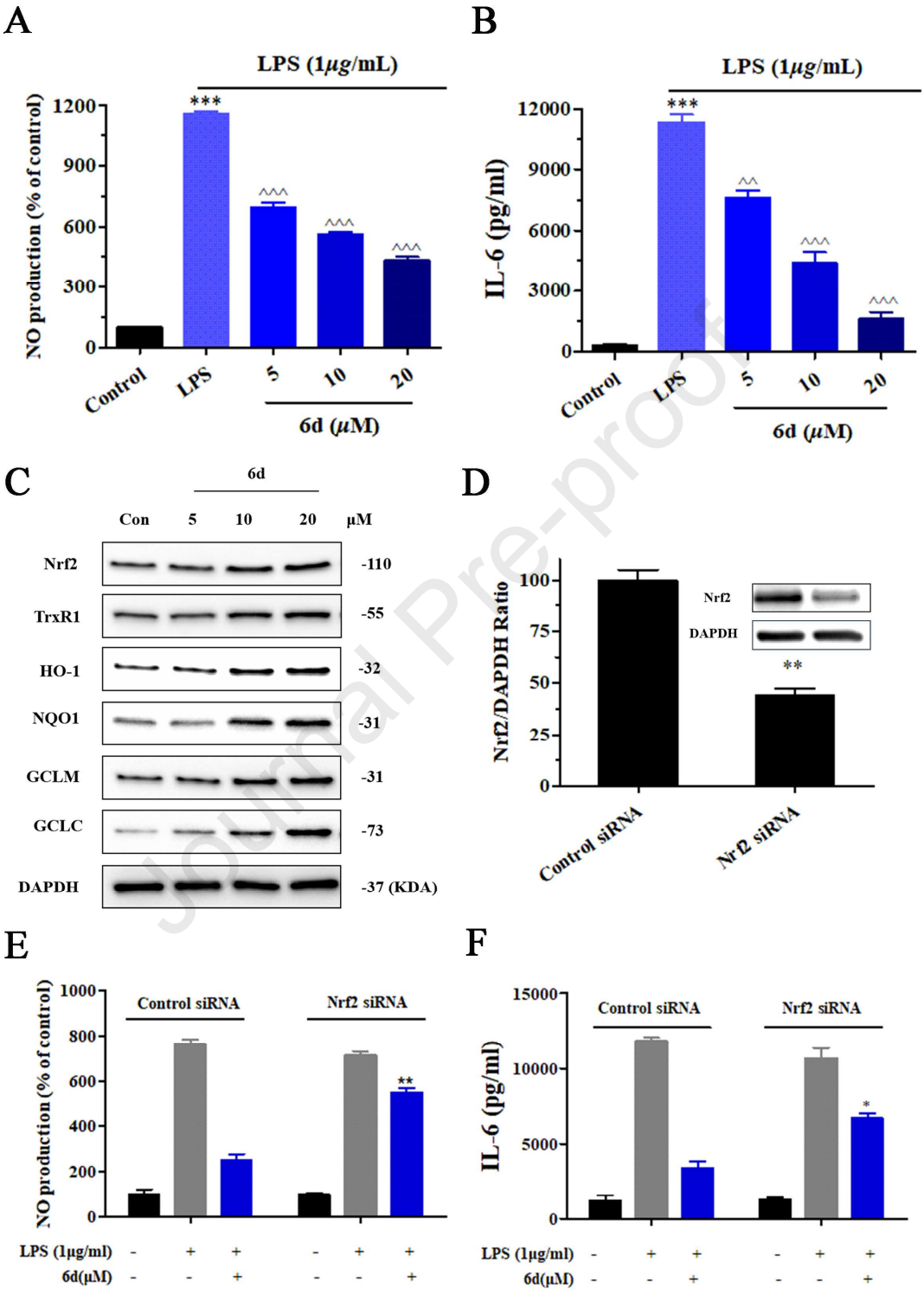

Figure 10. Contribution of Nrf2 to the anti-inflammatory effect of **6d**. (A) **6d** reduced the production of LPS-stimulated inflammatory mediators NO in BV2

microglia cells. (B) **6d** reduced the production of LPS-induced IL-6 in BV2 microglia cells. The levels of IL-6 were measured by ELISA kites. (C) **6d** dose dependently induced expression of Nrf2 and its downstream antioxidant proteins in BV2 microglia cells. (D) Nrf2 expression in Control siRNA- and Nrf2 siRNA-transfected BV2 microglia cells. (***p) ≤ 0.001 compared with the control group; (^^p) ≤ 0.01 and (^^^p) ≤ 0.001 compared with LPS-treated group. Transfection of BV2 microglia cells with Nrf2 siRNA reversed suppressive effects of **6d** (20 μM) on NO (E), IL-6 (F) production following LPS stimulation. **p≤0.01 and *p≤0.05 in comparison with control siRNA-transfected cells. Data are presented by mean ± SD (n = 3).

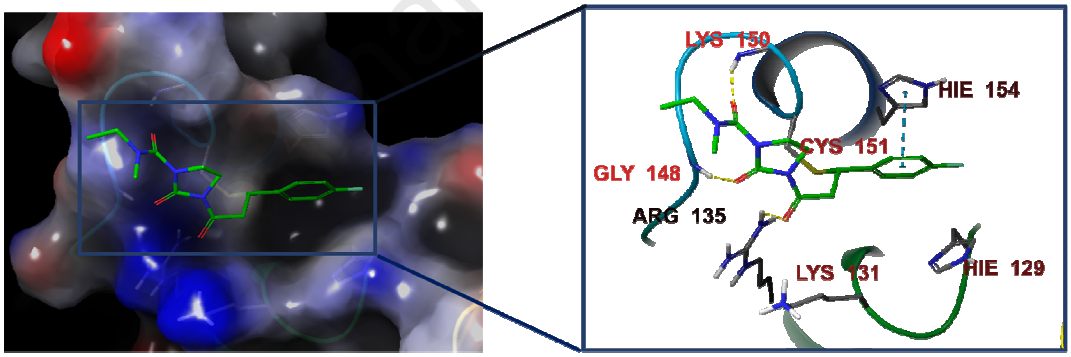

Figure 11. The docking model of **6d** with representative CYS in Keap1. 3D image of covalent docking between **6d** and CYS151 in the BTB domain (PDB: 4CXT).

Scheme 1. Synthesis of PL and its analogs[a]

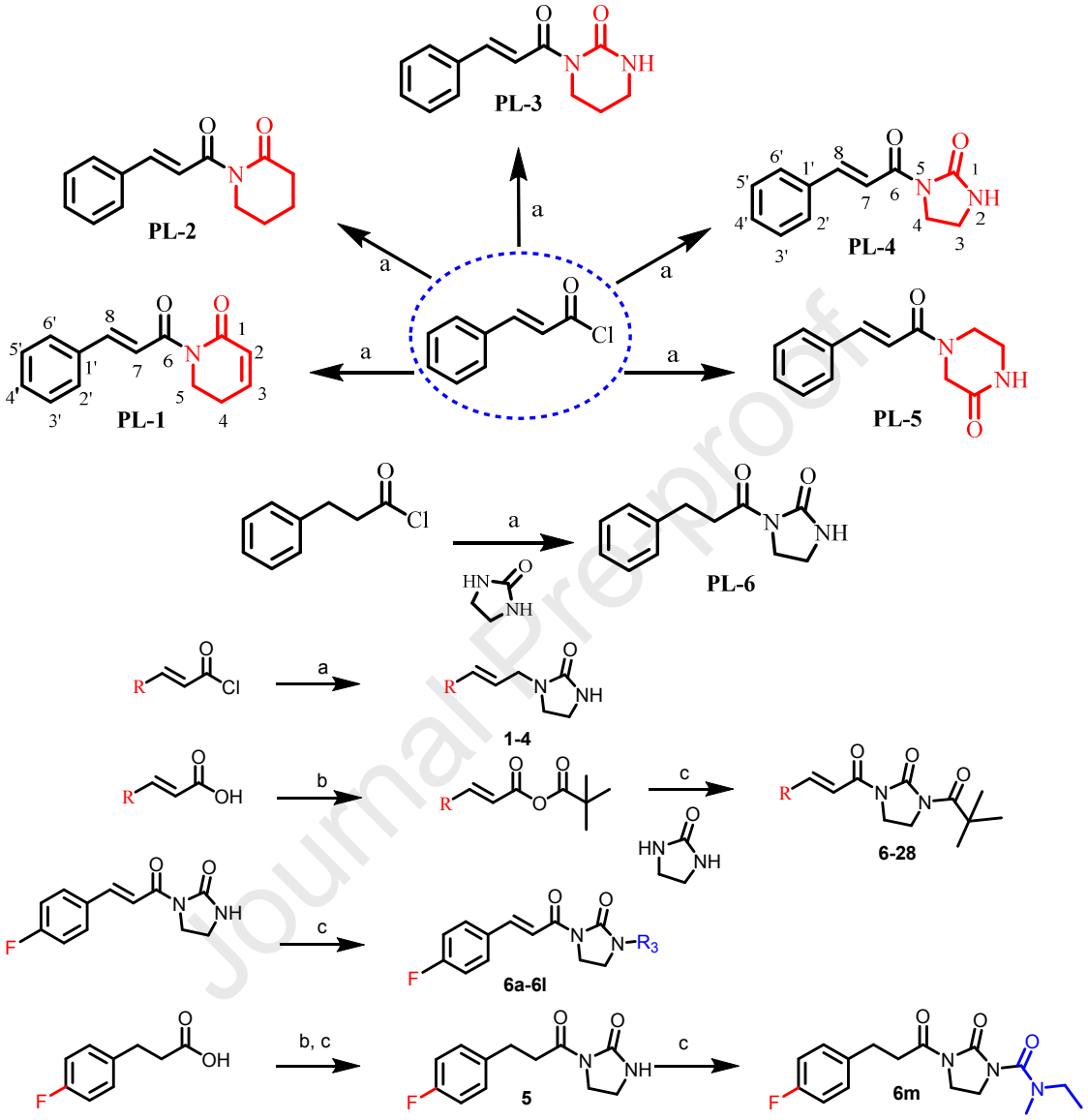

[a] Reagents and conditions: (a) NaH, THF, 0 °C, 30min; (b) Trimethylacetyl chloride, TEA, DCM, 0 °C, 30min; (c) NaH, DCM, 0 °C, 30min.

Journal Pre-proof

Journal Pre-proof

Highlights

- A series of piperlongumine derivatives were synthesized as neuroprotective agents by structure-based design.
- **6d** showed potent protection on PC12 cells against 6-OHDA- and H_2O_2-induced cell damage, alleviated ROS accumulation, mitochondrial dysfunction, Ca^{2+} influx, and cell apoptosis. Meanwhile, **6d** also showed good anti-inflammatory activity.
- Mechanism study proved that **6d** could activate keap1/Nrf2 signaling pathway, and upregulate downstream antioxidant enzymes such as NQO1, HO-1, GCLC, GCLM, and TrxR1.
- The parallel artificial membrane permeability assay indicated that **6d** would be potent to cross the blood-brain barrier.

Journal Pre-proof

Journal Pre-proof

Identification and optimization of Piperlongumine analogues as potential antioxidant and anti-inflammatory agents via activation of Nrf2

Limei Ji, Lailiang Qu, Cheng Wang, Wan Peng, Shang Li, Huali Yang, Heng Luo, Fucheng Yin, Dehua Lu, Xingchen Liu, Lingyi Kong*, Xiaobing Wang *

Jiangsu Key Laboratory of Bioactive Natural Product Research and State Key Laboratory of Natural Medicines, Department of Natural Medicinal Chemistry, School of Traditional Chinese Pharmacy, China Pharmaceutical University, Nanjing 210009, China

**Corresponding Authors.*

Tel/Fax: +86-25-83271405;

E-mail: xbwang@cpu.edu.cn (Xiaobing Wang); cpu_lykong@126.com (Lingyi Kong)

Journal Pre-proof

Declaration of interest statement

We declare that we do not have any commercial or associative interest that represents a conflict of interest in connection with the work submitted.